RSC Sustainability

ROYAL SOCIETY OF CHEMISTRY

PAPER

View Article Online
View Journal | View Issue

Cite this: *RSC Sustainability*, 2024, **2**, 4008

Aqueous-mediated DABCO and DABCO-ionic liquid catalysed synthesis of 3-acetylcoumarins: exploration by kinetic, electrochemical and spectroscopic studies

Arpita A. Shanbhag, Lokesh A. Shastri * and Samundeeswari L. Shastri

A more efficient, green and user-friendly approach for the synthesis of a combinatorial library of 3-acetylcoumarins from easily available ethylacetoacetate (EAA) and *o*-hydroxyaldehydes in water at room temperature was developed with excellent yields by modifying novel methods. The experimental method is facile and more economical than traditional methods, requiring no further product purification. Furthermore, the experimental conditions were optimized at the gram scale. The catalyst was reusable, resulting in excellent yields in a shorter time. Additionally, the by-product ethanol formed in the reaction was distilled out. Interestingly, the use of DABCO, DABCO-ionic liquids and DABCO salts as catalysts yielded excellent results (95–98%) in a shorter time. All products were identified by comparing their physical and spectroscopic data. The versatility of the developed green approach encouraged us to investigate the kinetics of the slowest step in the reaction and arrive at a rate law for the reaction. The kinetic and thermodynamic experimental results prompted us to undertake spectroscopic studies, including IR and ^{1}H NMR, which demonstrated that the catalyst initiated the mechanism. Additionally, cyclic voltammetry (CV), a key electroanalytical tool, showed both the spontaneity of the reaction and the tautomerism of EAA.

Received 12th August 2024
Accepted 23rd October 2024

DOI: 10.1039/d4su00465e

rsc.li/rscsus

Sustainability spotlight

Knoevenagel condensation is commonly used for the synthesis of 3-acetylcoumarins, where piperidine is employed as a base. However, this base is removed through an excess alcohol washing, during which a significant amount of soluble product may be lost, resulting in a reduced yield. Second, piperidine is toxic upon skin contact or inhalation, potentially causing severe skin burns and eye damage. Our focus is on developing a protocol to accelerate 3-acetylcoumarins synthesis using a green method. In this context, we envisioned the use of highly efficient catalysts (DABCO and DABCO-ionic liquid) that could be easily recovered and reused. The by-product is ethanol, which can be distilled under reduced pressure and reused when necessary. Remarkably, we achieved this reaction at room temperatures in very short time periods, and we verified the process using kinetic, electrochemical, and spectroscopic studies. So far, spectroscopic techniques have shown the tautomerism of EAA using various methods. Curiosity regarding EAA tautomerism and also the arrested form of tautomerism made us propose the use of the electrochemical technique CV, which is still reliable and not time consuming. The isolated products were more than 95% pure (no purification required). Our work emphasizes the importance of the following UN sustainable development goals: affordable and clean energy (SDG 7) and industry, innovation and infrastructure (SDG 9).

Introduction

Half of all known organic compounds are heterocycles, making this class of chemicals extremely significant. Indeed, the majority of vitamins, optoelectronics, pharmaceuticals, and several other natural goods are heterocycles. Benzopyrones represent an important class of heterocyclic compounds, of which benzo-α-pyrones, commonly called coumarins, are significant and involve the fusion of a pyrone ring with a benzene nucleus.[1] Vogel[2] first isolated coumarin from tonka beans. Although coumarin is a naturally active substance, its activity can be enhanced by combining it with various chemical moieties. Conventional methods for producing the coumarin nucleus include the Pechmann,[3] Knoevenagel,[4] Perkin,[5] Reformatsky,[6] and Wittig[7] condensation processes. Ongoing attempts have been made towards novel, practical and adaptable methods for synthesizing the coumarin nucleus with clear structural characteristics. Several modifications, including variations in the catalyst and reaction conditions, have been introduced to improve the efficacy of these classical reactions.[8] In recent years, versatile coumarin synthesis has been achieved through organopalladium intermediates.[9] Additionally, coumarins and their derivatives have been utilized as key

Department of Chemistry, Karnatak University, Dharwad, Karnataka 580 003, India. E-mail: drlashastri@kud.ac.in

components in a wide range of applications, including laser dyes,[10] fluorescent metal ion sensors,[11] solution dynamic probes,[12] and, more recently, organic sensitizers in high-efficiency dye-sensitized solar cells.[13]

For instance, derivatives of 3-acetylcoumarins have found numerous useful applications, including as fluorescence brighteners,[14] inhibitors of Zn corrosion in acidic media,[15] and in biological applications due to their various activities, such as antibacterial,[16] EGFR inhibition,[17] anti-breast cancer,[18] α-amylase inhibition,[19] antimycobacterial,[20] anti-inflammatory and analgesic,[21,22] and fluorescence dye properties.[23] According to previous studies, 3-acetylcoumarins have been synthesized using various catalysts,[24–30] with the various protocols having distinct advantages and disadvantages. Ultimately, chemists usually aim for new approaches that can offer more merits and less demerits, such as a workable procedure, high purity of product, good yield, and no effects on human health or the environment. Undoubtedly, there are a few advantages in the reported works, but there are more disadvantages too in terms of the usage of organic solvents for the reaction, excess usage of solvents for washing, usage of certain hazardous catalysts in the reactions that can cause health issues, and economic concerns about the more costlier catalyst and reagents used. However, many eco-friendly DABCO-based organocatalysts have been screened in organic synthesis, and these catalysts were found to show good to excellent performance in many organic reactions.[31]

Many methods have been reported, among which the Knoevenagel condensation is commonly used for the synthesis of 3-acetylcoumarins; however, piperidine is used as a base, which is removed by excess alcohol washing, which may also lead to the loss of soluble product and a reduction in the % yield. Other reported methods have similar disadvantages with product isolation and purification. Also, many reports have discussed the organic reaction mechanism *via* quantitative approaches. In recent years, qualitative approaches, such as electrochemical and spectroscopic methodologies, have yielded more authentic and impressive information about organic reaction mechanisms involving electron transfer. Such electron transfer can tune the thermodynamic or kinetic selectivity to form organic reactive intermediates. These intermediates can aid understanding the feasibility and kinetics of electron transfer, which clearly depends on the concentration of the reactant/catalyst.

Moreover, electroanalytical techniques offer a variety of ways to learn about the basic interactions, lifetimes, and reactivities that underlie redox reactions.[32] Nevertheless, the organic synthetic community has not embraced these tools extensively, with the majority of these techniques still being within the domain of analytical and physical chemists. This perspective seeks to provide an overview of the essential approaches for a synthetic chemist audience, with recommendations on how to get useful information on mechanistic issues. The information summarized herein will exemplify electrochemistry as a tool to choose the perfect catalyst, and for the identification and quantification of organic intermediate, kinetics, *etc.* A deeper comprehension of organic processes will be possible with knowledge of how these factors impact a mechanism, and could facilitate the creation of innovative synthetic strategies. Herein, we have come up with a user-friendly, green approach for the synthesis of 3-acetylcoumarins; in which water acts as a green solvent and DABCO-based green base and catalyst. A detailed investigation was carried out for the formation of 3-acetyl coumarin and also its mechanism was determined using kinetic, thermodynamic, cyclic voltammetry, and spectroscopic approaches.

Results and discussion

Optimization study

A green method involving the condensation of EAA (**1**) with *o*-hydroxyaldehydes (**2**) took place smoothly in the presence of diazabicyclo [2, 2, 2] octane (DABCO) as a base in water at room temperature, which resulted in the formation of 3-acetylcoumarins (**3**) in excellent yield (Scheme 2). As a model reaction, the condensation of **1** with **2a** to generate 3-acetylcoumarin (**3a**) was investigated (Scheme 1) using various bases to optimize the yield, and the obtained results are presented in Table 1. The reaction was relatively fast (~10–15 min) when 1 equiv. of DABCO was employed stoichiometrically. The other tested bases, like DBU (Table 1, entry 4) and DMAP (Table 1, entry 5), also gave good yields of the desired product **3a**. In contrast, MeONa (Table 1, entry 1), EtONa (Table 1, entry 2), and NaOAc (Table 1, entry 3) gave poor yields and needed a longer time. Thus, it is clear from the aforementioned experiments that the best yield of 3-acetylcoumarin **3a** could be obtained by employing DABCO as a green catalyst and water as a solvent.

Initially, the reaction was performed using various bases (Table 1) to avoid the use of piperidine as a base in the reaction, and water as medium, as a green solvent, instead of alcohol and also other solvents (DCM, toluene, 1,4-dioxane). Studies of the effects on the reaction from the excess usage of bases (alkoxides, acetates, and *tert*-amines) and varying the time duration were done in water as a medium at room temperature, with heating applied as needed. In the case of sodium methoxide, the formation of the product was noticed, but the reaction could not be completed even after increasing the equivalence of

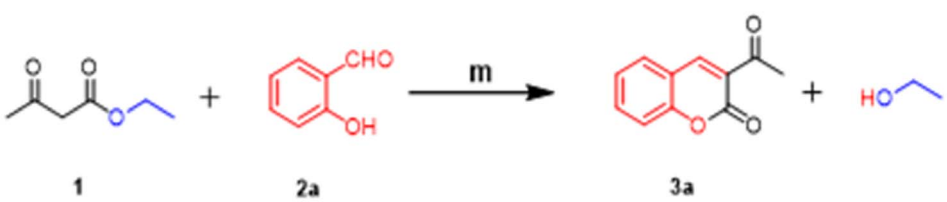

Scheme 1 Screening of different bases/catalysts* in the model reaction between EAA **1** and salicylaldehyde **2a**.

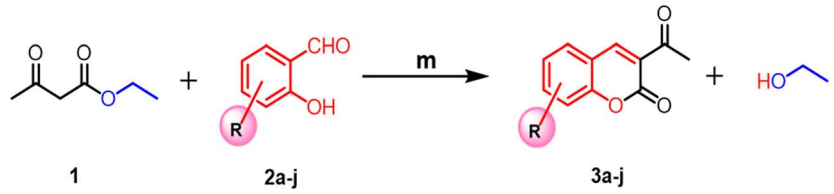

2a: R = H
2b: R = 4-OMe
2c: R = 3-Br-5-Cl
2d: R = 5-OH
2e: R = 4-N(Et)$_2$
2f: R = 3-OMe
2g: R = 2-OH-naphthaldehdye
2h: R = 4-Br
*__2i:__ R= 5-NO$_2$
*__2j:__ R= 3-OMe-5-NO$_2$

Reagents and conditions: (m) DABCO or DABCO- ionic liquids, water, r.t.

Scope of o-hydroxyaldehydes

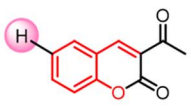

3a

98%
(lit.,[24b] 119 °C)

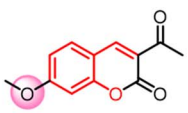

3b

97%
(lit.,[36a] 152 °C)

3c

97%
(lit.,[36b] 150 °C)

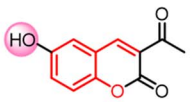

3d

95%
(lit.,[36c] 185 °C)

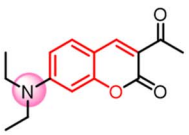

3e

96%
(lit.,[36d] 153 °C)

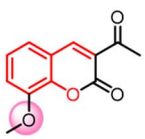

3f

96%
(lit.,[36d] 165 °C)

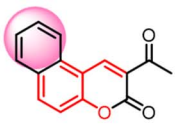

3g

98%
(lit.,[36d] 183 °C)

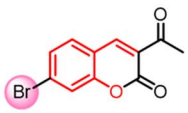

3h

97%
(lit.,[36e] 215 °C)

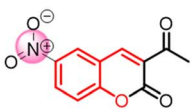

3i

27%, *71%
(lit.,[36f] 195 °C)

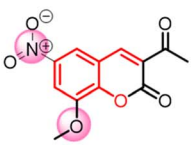

3j

30%, *75%
(lit.,[36f] 215 °C)

Scheme 2 Scope of the reaction of *o*-hydroxyaldehydes **2a–h** with EAA 1 employing different catalysts. % Yield taken in the gram scale and melting point in °C. *Heating (65–70 °C), **literature value.[24b,36a–f]

MeONa as well as raising the temperature (~95 °C), and the isolated product was obtained in a yield of less than 60% (Table 1, entry 1). Similarly, sodium ethoxide resulted in almost the same yield (Table 1, entry 2); whereas sodium acetate as a base showed much less product formation even at higher temperature and with a longer reaction time (Table 1, entry 3). In search

Table 1 Optimization of the synthesis of 3-acetylcoumarin using various bases (Scheme 1)

Entry	Bases/catalysts	Time	Yield%
1	MeONa	2–3 h	<60
2	EtONa	2–3 h	<60
3	NaOAc	2–3 days	<50
4	DBU	15–20 min	75
5	DMAP	15–20 min	78
6	DABCO	10–15 min	95
7	[H-dabco][Cl]	15–20 min	98
8	[H-dabco][OAc]	20–25 min	85
9	DABCO-CuCl	15–20 min	95
10	DABCO-CuI	15–20 min	96

for new catalyst, previous literature reports informed us that most of the 3-acetylcoumarins were obtained using secondary/*tert*-amine bases other than water as a solvent. Therefore, keeping in mind the solubility of the base in water, we performed the reaction in H_2O with a catalytic quantity of DBU as the base. Surprisingly, the results of the reaction were quite excellent, and the reaction proceeded smoothly with a good yield within 20 min at room temperature (Table 1, entry 4). Similarly, DMAP (Table 1, entry 5) also showed almost the same results. Further screening was performed using DABCO, with excellent product formation in a shorter time with an isolated yield of more than 95% (Table 1, entry 6). The use of DABCO showed excellent results for the synthesis of 3-acetylcoumarin derivatives, compared to DBU and DMAP.

DABCO-based catalyst

Further, the DABCO-based catalyst was explored by using a modified DABCO-ionic liquid and DABCO salts for the synthesis of the title compounds. In view of previous studies, the effects of ionic liquids in certain reactions are believed to be very interesting; hence to evaluate the profile of ionic liquids, [H-dabco][AcO] and [H-dabco][Cl] were studied in condensation reactions in the present work. These ionic liquids were synthesized according to the literature reports.[33] As we can see from the results summarized in Table 1, the condensation reaction of EAA (**1**) with *o*-hydroxyaldehyde (**2a**) in water at room temperature with the DABCO-ionic liquid used as the catalyst was found to be excellent. The [H-dabco][Cl]-catalyzed (Table 1, entry 7) reaction showed extremely good results in terms of yield and reaction time, whereas the [H-dabco][AcO] catalyst (Table 1, entry 8) showed a lower yield and required a little more time.

However, apart from DABCO-ionic liquids, we intended to investigate whether it was possible to conduct the reaction using DABCO–CuX complex. The novel DABCO–CuX complex[34] was synthesized by grinding a 1 : 1 equivalent ratio of DABCO and CuX and the using this complex for the synthesis of 3-acetylcoumarin (**3a**) in water as a medium using EAA (**1**) with *o*-hydroxyaldehyde (**2a**) at room temperature. Interestingly, the DABCO–CuX complex-catalyzed condensation reaction showed quite excellent yields (≃96%, Table 1, entries 9–10), which were nearly similar to those obtained with DABCO-ionic liquids.

Recovering of ethanol

The solid obtained in experiments based on the model reaction was filtered thoroughly and washed with water to remove excess DABCO-based catalyst. The filtrate containing the water-soluble DABCO catalyst and by-product ethanol were separated by distillation under reduced pressure. The experiment was conducted in the gram scale in order to calculate the by-product

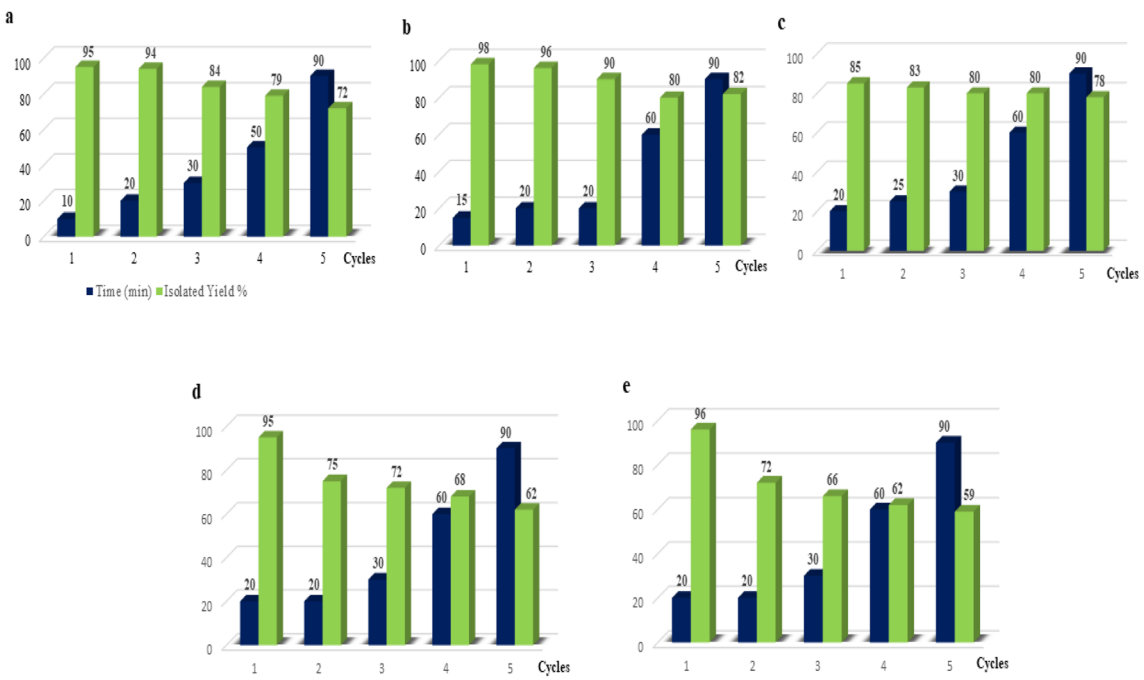

Fig. 1 Reuse of the catalysts (a) DABCO, (b) [H-dabco][Cl], (c) [H-dabco][AcO], (d) DABCO–CuCl, and (e) DABCO–CuI in the model reaction between EAA **1** and salicylaldehyde **2a** in the presence of water.

ethanol. Salicylaldehyde **2a** (5 g, 1 eq., 40.95 mmol) upon reaction with EAA **1** (5.340 g, 1 eq., 38.40 mmol) in the presence of DABCO catalyst gave 1.490 g (97%) ethanol as a by-product.

Reusability of the DABCO-based catalyst

The DABCO, DABCO-ionic liquids, and DABCO-complex catalyst screening results inspired us to extend our investigations to study the reusability of these catalysts for the reaction. As a model reaction EAA (**1**) reacted with salicylaldehyde (**2a**) in water using one equivalent of DABCO to give product **3a** in a 95% yield in the first cycle (Fig. 1a). The second cycle gave almost the same percentage yields. However, upon increasing the time duration from 30–90 min for the third to fifth cycle, the percentage (%) yield formation decreased from 84% to 72%.

The reusability results based on the experimental observations for the modification of DABCO into DABCO-ionic liquids [H-dabco][Cl] and [H-dabco][AcO] are summarized in Fig. 1b and c, respectively. The reuse of the [H-dabco][Cl] ionic liquid was explored for the synthesis of 3-acetyl coumarin derivatives *via* eco-friendly conditions by taking EAA (**1**) and salicylaldehyde (**2a**) at room temperature. Surprisingly, we noticed that the product formation of **3a** was 98% and 96% I the first two cycles, respectively (Fig. 1b, cycle 1 and 2). Further catalyst reusability experiments were conducted for up to five cycles, ad it was found that the percentage of product formation decreased. For, [H-dabco][AcO] ionic liquids, smooth progress of the reaction was noticed for a certain period of time, *i.e.* 20–25 min, after which no progress of the reaction was observed, even with prolonged stirring and about 15–20% of the starting material remained, with the results shown in Fig. 1c. From these results, it could be observed that the ionic liquid system [H-dabco][Cl] was superior to [H-dabco][AcO] in terms of yield and time.

Further, the catalyst reusability investigations were extended by modifying DABCO to DABCO–CuX salts ($X = Cl, I$), in order to understand the efficiency of DABCO, and the reaction was then performed using the DABCO–CuX catalyst at room temperature in water with **1** and **2a**. More interestingly, the reaction proceeded very smoothly within 20 min with a 95% conversion of the target molecule in the first cycle; while, in the second to fifth cycles, the efficiency of the catalyst was drastically reduced (Fig. 1d and e).

The catalyst reusability experimental investigation results indicated that DABCO and DABCO-ionic liquids are extremely good for clean synthesis of the title compounds compared to DABCO–CuX salts.

Catalytic efficiency

The catalytic efficiency of the DABCO-based organocatalysts was screened. A graph of the variation of the catalytic efficiency as a function of reuse times (cycles) is shown in Fig. 2. The variation in catalytic efficiency was affected by certain key properties, such as hydration effect,[35a,b] solvation effect,[35c] viscosity,[35d] and hydrogen bonding[35e,f], leading to a decrease in the catalytic activity.

Scope for methodology

To test the generality of the condensation and to realize the synthesis of a small combinatorial library of 3-acetylcoumarins (**3a–j**) from EAA (**1**) and different *o*-hydroxyaldehydes (**2a–j**), we aimed to furnish the title compounds in good yields by using

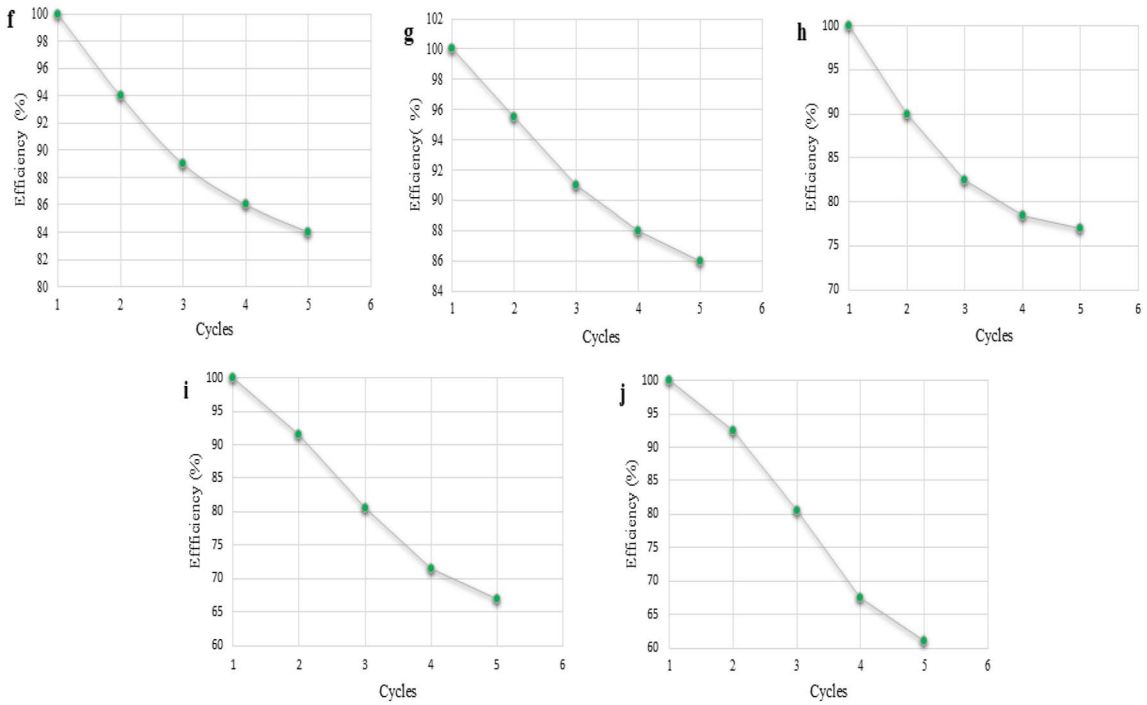

Fig. 2 Variation of the catalytic efficiency as function of the catalyst reuse times (cycles) for (f) DABCO, (g) [H-dabco][Cl], (h) [H-dabco][AcO], (i) DABCO–CuCl, and (j) DABCO–CuI in the model reaction between EAA **1** and salicylaldehyde **2a** in the presence of water.

DABCO and DABCO-ionic liquids as a catalyst and water as a medium at room temperature (Scheme 2). Based on our experimental observations, the electron-releasing or -withdrawing group on *o*-hydroxyaldehydes played a major role; mainly, the electron-donating group led to excellent yield. In the case of strong electron-withdrawing groups, such as nitro substituent *para*-to the hydroxy group of *o*-hydroxyaldehydes, the reaction took longer, with a low yield (≃30% and 2–3 days) at room temperature, while under heating (65 °C-70 °C), the reaction gave a 75% yield within 2–3 h. A comparative investigation was made for the synthesis of 3-acetyl coumarins and the results are shown in Table 2. These synthesized compounds are utilized in various applications, such as material science and medicinal chemistry.

Experimental determination of the reaction mechanism

The versatility of the green approach encouraged us to understand the reaction mechanism, which was faster and cleaner

Table 2 Comparison of methods for the synthesis of 3-acetylcoumarin with present work

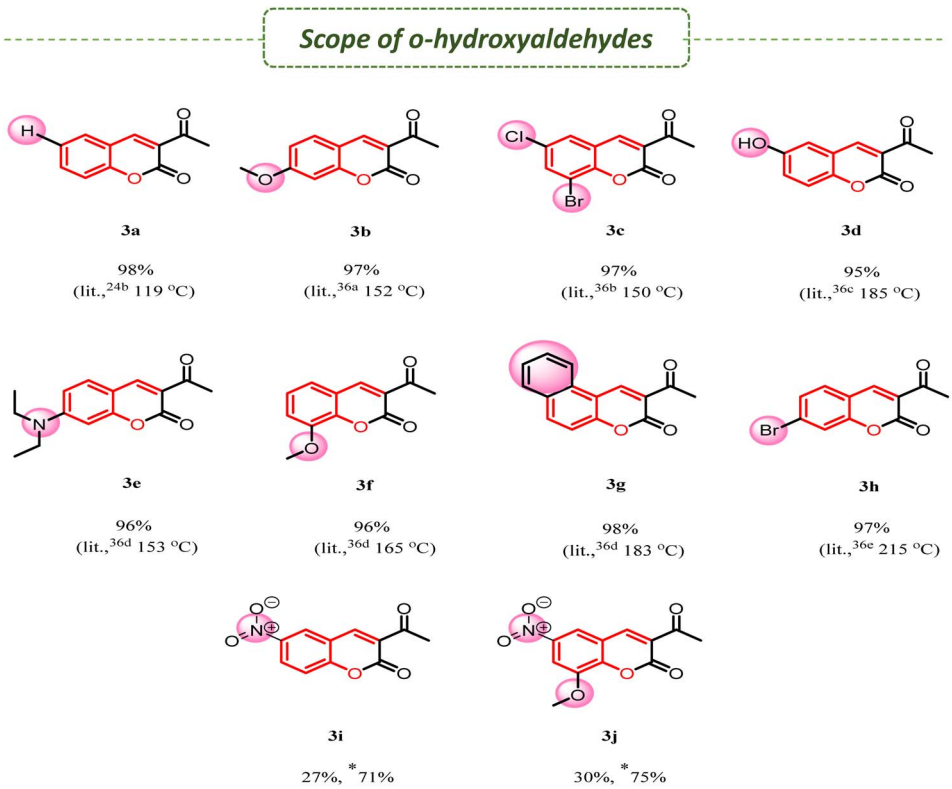

	Reaction conditions	Solvent	Catalyst	Time (min)	Yield (%)	Reference
1	Stirring, r.t	Ethanol	Piperidine	20	83.5	24a
2	Microwave irradiation, 136 °C	Ethanol	Piperidine	6	88	24b
3	Reflux	Ethanol	Piperidine	30	92	24c
4	Microwave irradiation	Solvent free	Piperidine	—	92.6	24d
5	Continuous-flow units, 25–130 °C	Ethyl acetate	Piperidine	—	72	24e
6	Ultrasound irradiation, 45 °C	Solvent free	$MgFe_2O_4$ nanoparticles	10	92–96	25a
7	Microwave irradiation 120 °C or thermal, 100 °C	Solvent free	ZnO nano	5–9, 36–72	90	25b
8	Stirring, 35–40 °C	Ethanol	$PhI(OAc)_2$	30–60	82–92	26a
9	Stirring, 60–80 °C	Dimethyl formamide	$Fe_3O(BPDC)_3$ containing *tert*-butyl hydroperoxide	180	65–96	26b
10	Stirring, 90 °C	2.16% H_2O	[MMIm][MSO_4] containing L-proline	15	99	27a
11	Stirring, 25–30 °C	Water	Choline chloride	20–45	90	27b
12	Stirring, 60–80 °C	Solvent free	L-proline	30	98	28a
13	Stirring, r.t −80 °C	Water	L-lysine	2880 (48 h)	35–87	28b
14	Stirred, 80 °C	Solvent free	CSA	210 (3.5 h)	88	29
15	Reflux	Ethanol	HPA	120 (2 h)	50–98	30
*	Stirring, r.t. (present work)	Water	DABCO and DABCO-based catalysts	10–20	95–98	—

compared to earlier reported methods. However, no such investigation was found in the literature involving DABCO organocatalyzed reactions. Hence, in order to gain an insight into the effects of the organocatalyst DABCO, we carried out a certain approach to determine the kinetic rate, and thermodynamic activation parameters in the aqueous phase. Also, a spectroscopic approach was applied for identification of the product formation quantitatively and qualitatively. The obtained experimental evidence supported the use of a stoichiometric amount of substrates, and the effects of the solvent, catalyst, temperature, and reaction time.

UV method

The absorption spectra of the reaction mixtures were measured at different concentrations of the organocatalyst DABCO, water as a solvent, and also both the reactants EAA (**1**) and salicylaldehyde (**2a**) under standard conditions. The results obtained from the absorption spectra are presented in Tables 3–5 and the reaction profile diagrams are plotted as the OD *vs.* time in Fig. 3–5.

Effect of water on the rate of reaction

To validate the reaction, initially the experiment was conducted using an equimolar ratio of both reactants (EAA (**1**), salicylaldehyde (**2a**)) and also DABCO catalyst as 1 eq. (Table 3, entry 1) in 10 ml of water. From the experimental results, the reaction began in the 37th min and was completed in 300 min, as monitored continuously by a UV spectrometer and TLC (Fig. 3A). Subsequently, the experiment was performed by reducing the water volume to 5 ml and 1 ml (Table 3, entries 2 and 3). The obtained results were quite excellent in the case of 1 ml water, and the reaction was completed in 10 min (Fig. 3C); while the reaction in 5 ml water needed 120 min for completion(Fig. 3B).

The aforementioned experiment illustrates that lowering the volume of water increased the reaction rate. Moreover, in raising the water volume out of our curiosity to up to 20–50 ml, it was observed that the reaction happened but took much longer for completion of the reaction (3–5 days), as monitored using TLC. Since, the solvation effect could explain the drastic drop in the reaction rate,[37] the rate-determining step does not take water concentration into consideration.

Table 3 Effect of the concentration of [DABCO] and [H_2O] in the synthesis of 3-acetylcoumarin from salicylaldehyde (1 eq.) with EAA (1 eq.) at 303 K

Entry	DABCO (eq.)	Water (ml)	Time (min)	Rate
1	1	10	300	0.01
2	1	5	120	0.03
3	**1**	**1**	**10**	**0.04**
4	0.5	1	22	0.03
5	0.1	1	28	0.03

Table 4 Effect of salicylaldehyde concentration on the reaction (EAA (1 eq.) + DABCO (1 eq.) + water (1 ml))

Entry	Sal (eq.)	K	Log[k]	Log[R]
1	1	0.0403	−1.3947	−0.3033
2	0.5	0.0276	−1.5591	−0.6043
3	0.1	0.0076	−2.1191	−1.3036

Table 5 Effect of EAA concentration on the reaction (Sal (1 eq.) + DABCO (1 eq.) + water (1 ml))

Entry	EAA (eq.)	k	Log[k]	Log[R]
1	1	0.0403	−1.3947	−0.3035
2	0.5	0.0111	−1.9547	−0.6047
3	0.1	0.0086	−2.0655	−1.3036

Effect of DABCO on the rate of reaction

Moreover, the above investigation encouraged us to explore the reaction by varying the ratio of the organocatalyst DABCO in 1 ml of water while keeping the other reactants constant (Table 3, entries 4 and 5). The experimental results revealed that the rate of reaction was independent of the base concentration. Therefore, the base concentration term was not included in the rate-determining step. From the UV spectroscopic data, we could conclude the rate of reaction as $r_{1eq.} \geq r_{0.5eq.} \geq r_{0.1eq.}$ (Table 3, entries 3–5; Fig. 3C–E). Although, there was no catalyst involvement in the rate-determining step, it is essential for the reaction as it initiates as well as it controls the tautomerism of EAA, thereby starting an irreversible reaction by forming complex **X** with DABCO (Fig. 7, Phase Ib). The more preferred irreversible reaction step of EAA-DABCO complex formation **X** was confirmed using cyclic voltammetry (Fig. 12).

Effect of salicylaldehyde and EAA concentration on the rate of reaction

In the catalytic domain, both the salicylaldehyde (**2a**) and EAA (**1**) concentration effects on the rate of the reaction were tested. In the case of salicylaldehyde, the rate of reaction increased with the increase in concentration of salicylaldehyde while keeping the concentrations of the other species constant. Similarly, when the EAA concentration was increased while keeping the concentrations of the other species constant, the rate of reaction also increased. From the UV spectroscopic data, we could conclude that the rate of reaction for salicylaldehyde was $r_{1eq.} > r_{0.5eq.} > r_{0.1eq.}$ (Table 4, entries 1–3; Fig. 4F–H); and for EAA as $r_{1eq.} > r_{0.5eq.} > r_{0.1eq.}$ (Table 5, entries 1–3; Fig. 5M–O). Fig. 4I–K and Fig. 5P–R display the linear regression plot between the OD *vs.* time for the reaction. The correlation coefficients of the model reaction were observed as 0.9993, 0.9993, and 0.9996 for different concentration of salicylaldehyde with slopes of 0.0403, 0.0276, and 0.0076. Similarly, the correlation coefficients of the model reaction were observed as 0.9983, 0.9959, and 0.9989 for the different concentrations of EAA with slopes of 0.0403, 0.0111, and 0.0086. Fig. 4L and 5S illustrate the order of reaction from the plot of log(reactant) *vs.* log(k) for varying

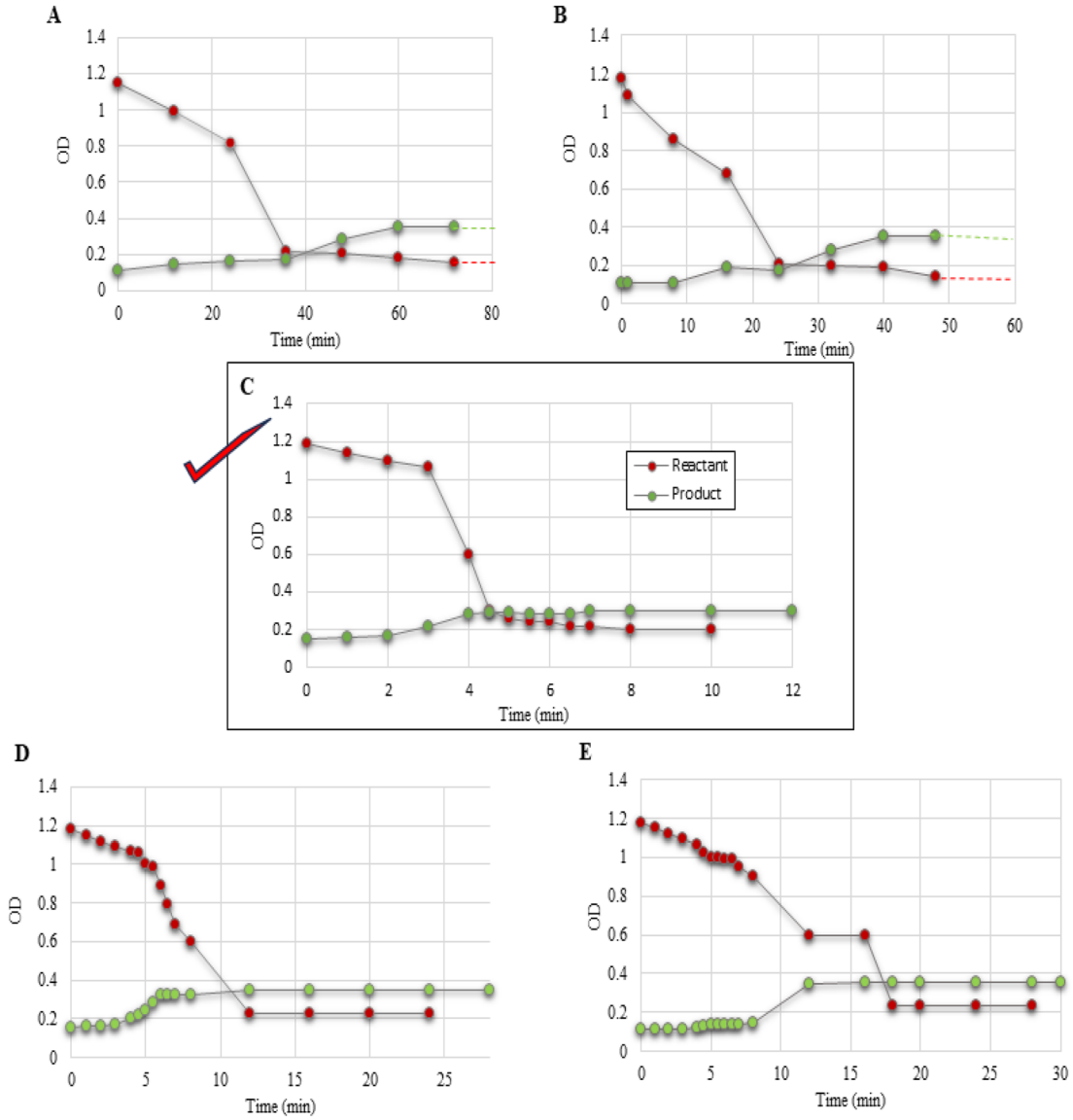

Fig. 3 Reaction profiles (A–E) for the experiments conducted and listed as entries 1–5 in Table 3. The solid red dots indicate the reactant and green dots are for the product.

concentrations of salicylaldehyde and EAA with average slopes of 0.9008 and 0.8308 and a correlation coefficient of 1.

Rate law derivation

A kinetic investigation would typically involve the postulation of likely mechanisms and a comparison between the observed rate expression and those anticipated from theoretical approaches. It is possible to exclude from consideration any mechanisms that are incompatible with the reported kinetics.[38]

Based on the kinetic experimental observations, the reaction mechanism is proposed in Fig. 7. The rate law for reaction was derived by means of spectroscopic data; wherein, the formation of intermediate **Y** was shown to be the slowest rate-determining step (Fig. 7, Phase II). Also, by UV method, it was confirmed that only the concentration of salicylaldehyde and EAA were involved in the rate-determining step. To illustrate the development of a kinetic expression from a postulated reaction mechanism (Fig. 7), we know that the slowest step is the rate-determining step for a reaction, and the rate equation can be written as,[39]

$$\text{Rate} = k_2[\text{ED}][\text{Sal}]$$

Where k_2 = rate constant at Phase II.

[ED] = EAA–DABCO complex

$$[\text{Sal}]^t = [\text{Sal}]^f$$

Where $[\text{Sal}]_t$ = concentration of salicylaldehyde at time 't'.

$[\text{Sal}]^f = [\text{Sal}]$, where $[\text{Sal}]^f$ means salicylaldehyde free from all components of reactions

$$[\text{EAA}]^t = [\text{EAA}]^f + [\text{ED}]$$

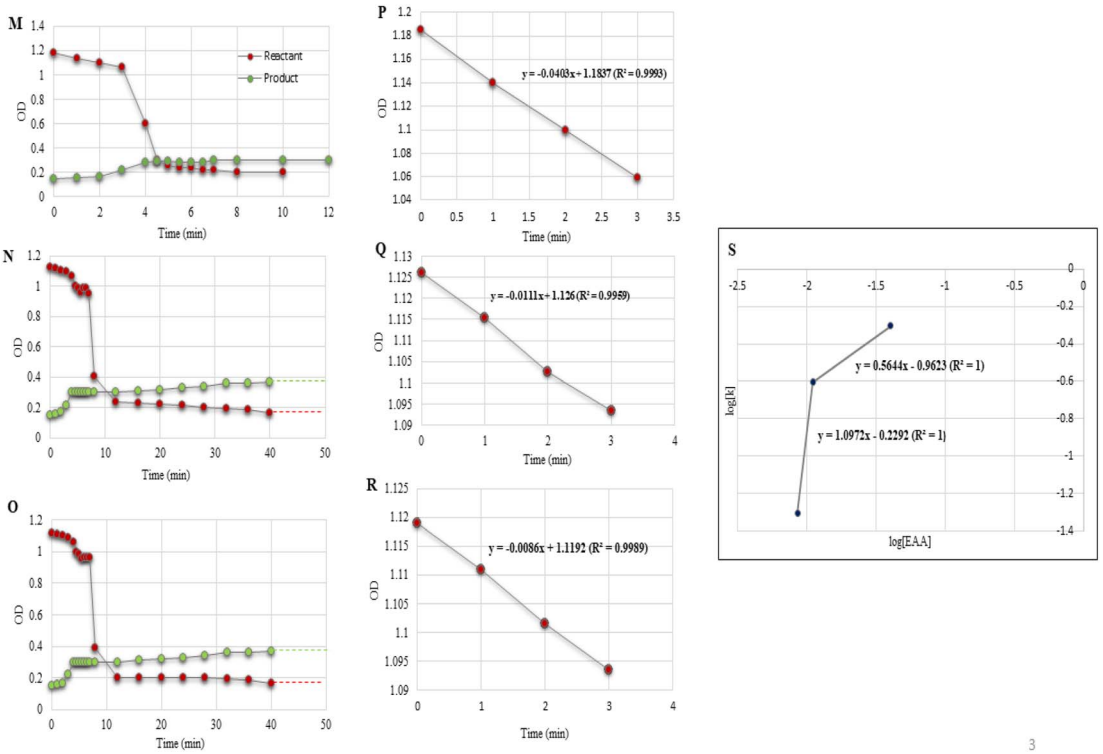

Fig. 4 (F–H) Reaction profiles for experiments conducted and listed as entries 1–3 in Table 4. (I–K) Regression plots of OD *vs.* time. (L) Order plot: log[*k*] *vs.* log[Sal]. Solid red dots indicate the reactant and green dots are for the product.

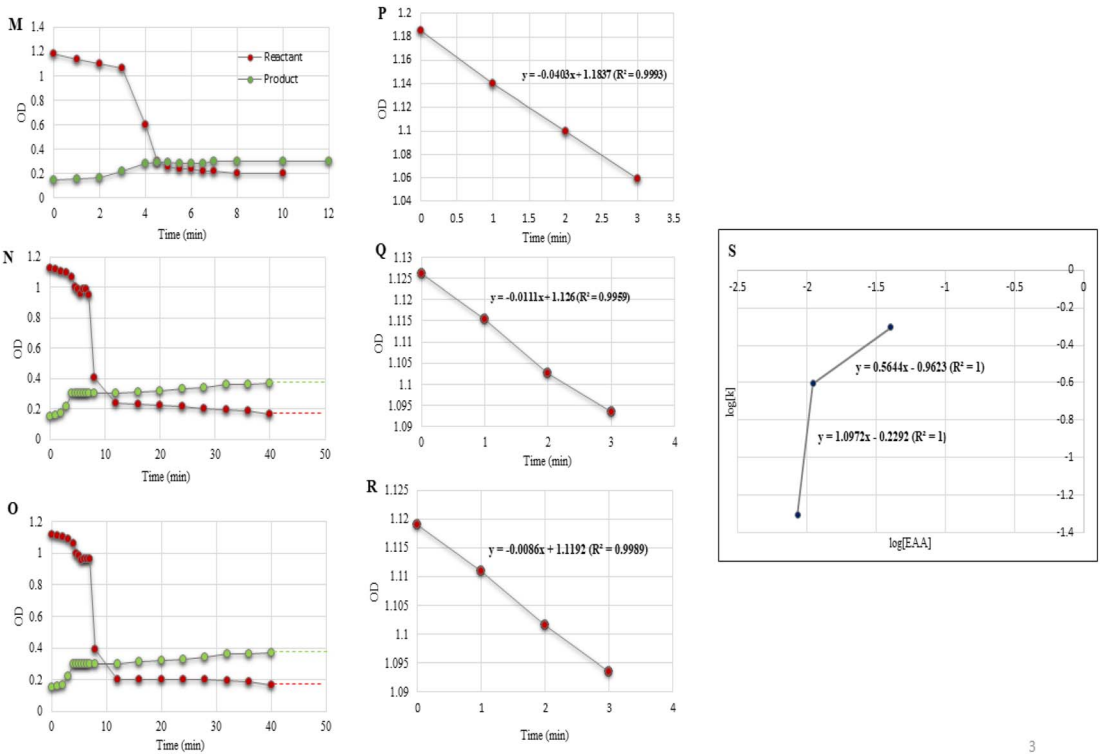

Fig. 5 (M–O) Reaction profile for experiments conducted and listed as entries 1–3 in Table 5. (P–R) Regression plots of OD *vs.* time. (S) Order plot: log[*k*] *vs.* log[EAA]. Solid red dots indicate the reactant and green dots are for the product.

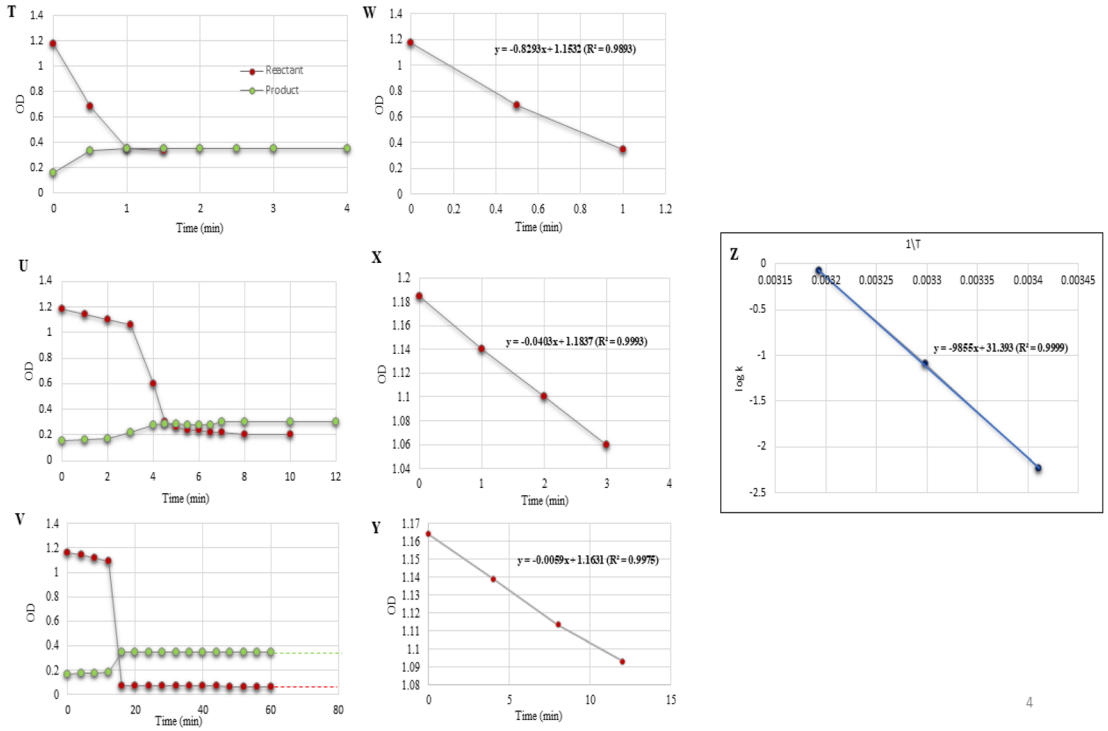

Fig. 6 (T–V) Reaction profiles for the experiments conducted and listed as entries 1–3 in Table 6. (W–Y) Regression plots of OD *vs.* time. (Z) Plot of log[*k*] *vs.* [1\T] in determining the activation parameters. The solid red dots indicate the reactant and the green dots are for the product.

$$= [\mathrm{EAA}]^{f} + k_1[\mathrm{EAA}]^{f}$$

Where $[\mathrm{EAA}]^{t}$ = concentration of EAA at time '*t*'.

$[\mathrm{EAA}]^{f}$ = [EAA], where $[\mathrm{EAA}]^{f}$ means EAA free from all components of reactions

$$[\mathrm{EAA}]^{t} = [\mathrm{EAA}]^{f}\{1 + k_1\}$$

Where k_1 = rate constant at Phase I

$$[\mathrm{ED}] = [\mathrm{EAA}]^{t} - [\mathrm{EAA}]^{f}$$

$$\mathrm{Rate} = k_2\{[\mathrm{EAA}]^{t} - [\mathrm{EAA}]^{f}\}[\mathrm{Sal}]$$

$$= k_2\ \{[\mathrm{EAA}]^{t} - [\mathrm{EAA}]^{t}/(1 + k_1)\}[\mathrm{Sal}]$$

$$= k_2\{1 - (1/1 + k_1)\}[\mathrm{EAA}]^{t}[\mathrm{Sal}]$$

$$= k_2\{k_1/1 + k_1\}[\mathrm{EAA}]^{t}[\mathrm{Sal}]$$

$$= \{k_1k_2/(1 + k_1)\}[\mathrm{EAA}][\mathrm{Sal}]$$

$$\mathrm{Rate} = k[\mathrm{EAA}][\mathrm{Sal}] \text{ where, } k = \{k_1k_2/(1 + k_1)\}$$

The reaction orders were calculated from the slopes of $\log(k_{obs})$ *vs.* log(concentration) plots by varying the concentrations of salicylaldehyde (Table 4, entries 1–3; Fig. 4L) and EAA (Table 5, entries 1–3; Fig. 5S) while keeping all the other conditions constant.

Under optimized experimental conditions, the rate law can be written as, $R \propto [\text{salicylaldehyde}]^{0.9008}\ [\mathrm{EAA}]^{0.8308}$ order = 0.9008 + 0.8308 = 1.732.

Effect of temperature

The rate of reaction was measured at different temperatures, considering the same reaction conditions as chosen for the spectroscopic studies. Once again, the UV spectroscopic data allowed concluding the rate of reaction as $r_{40} > r_{30} > r_{20}$, *i.e.* 0.8293 > 0.0403 > 0.0059 mol^{-1} L s^{-1} (Table 6, entries 1–3; Fig. 6(T–V)). Fig. 6(W–Y) display linear regression plots between the OD *vs.* time for the reactants. The correlation coefficients of the model reaction were observed as 0.9893, 0.9993, and 0.9975 for different temperatures with slopes of 0.8293, 0.0403, and 0.0059, respectively. With every 10 °C raise in temperature, the rate of the reaction increased by $r_{40} > r_{30}$; while the rate of reaction decreased with every 10 °C drop in temperature by

$$r_{30} > r_{20}.$$

Table 6 Effect of temperature on the synthesis of 3-acetyl coumarin using Sal (1 eq.) + EAA (1 eq.) + DABCO (1 eq.) + water (1 ml) in determining the activation parameters

Entry	Temperature (K)	$(1/T) \times 1000$	*k*	Log*k*
1	313	3.193	0.8293	−1.859
2	303	3.298	0.0403	−3.172
3	293	3.411	0.0059	−4.007

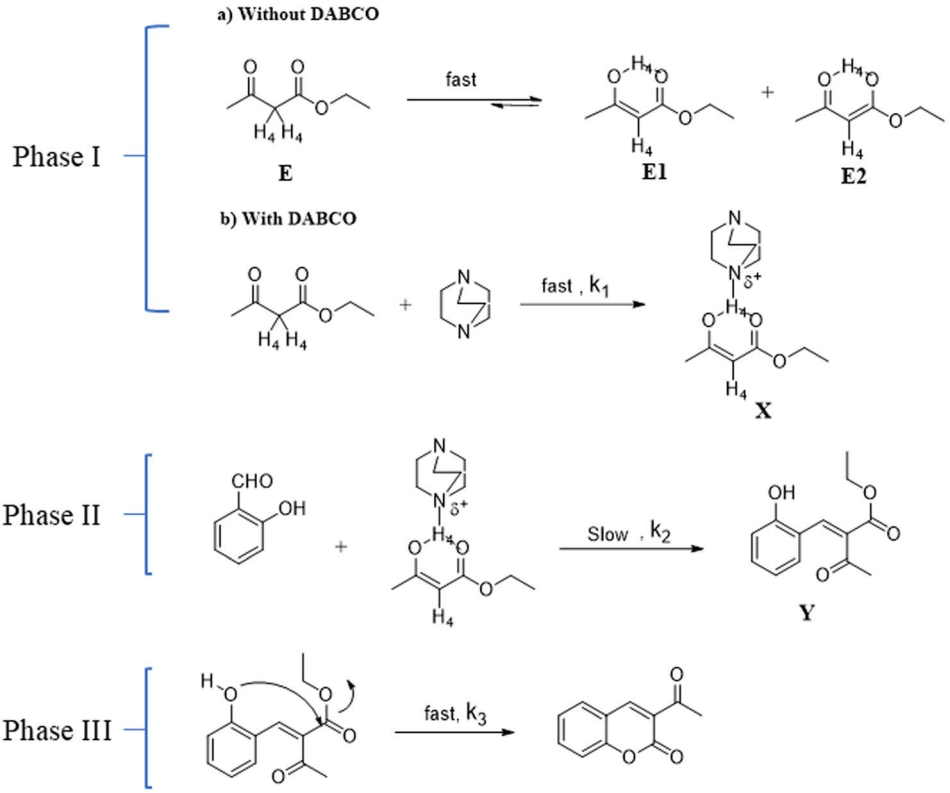

Fig. 7 Proposed reaction mechanism.

A detailed thermodynamic analysis of the activation parameters for the synthesis of 3-acetyl coumarin was performed and the activation parameters obtained from the slopes of $\log k_{obs}$ *vs.* $1/T$ plots by varying the temperature [Table 6, Fig. 6Z] for the model reaction salicylaldehyde (1 eq.), EAA (1 eq.), DABCO (1 eq.), and water (1 ml), as shown in Table 6, entries 1–3, and Fig. 6Z. Further, the activation parameters were also calculated for the slowest step of the reaction, and the activation energy was found to be E_a = 44.95 kcal mol^{-1}. Similarly, the other activation parameters were also calculated and provided in Table 7. In the table, the positive $\triangle S^{\#}$ indicates that the EAA–DABCO complex was more ordered/stable than the intermediate, while the positive $\triangle H^{\#}$ proves the condensation reaction was endothermic and the positive $\triangle G^{\#}$ shows the non-spontaneity of the slowest step.

Spectroscopy and cyclic voltammeter evidence

The kinetic and thermodynamic experimental results prompted us to undertake investigations utilizing electrochemical techniques, such as cyclic voltammetry (CV) and spectrochemical analysis, as these tools can help instantly provide more information on the spontaneity effect of a catalyst on the rate of a reaction.

Table 7 Activation parameters with respect to the slowest step of the reaction (E_a = 44.95 kcal mol^{-1})

	Values		
Parameters	313.16 K	303.16 K	293.16 K
$\Delta H^{\#}$ (kcal mol^{-1})	44.32	44.34	44.36
$\Delta S^{\#}$ (cal K^{-1} mol^{-1})	74.39	73.17	74.45
$\Delta G^{\#}$ (kcal mol^{-1})	21.03	22.16	22.54

IR spectra and ^{1}H NMR: a time-dependent study

Many methods have been adapted for clarifying the reaction mechanism, including spectroscopy for studying the reaction mechanism for homogeneous organic reactions. Spectroscopy plays a crucial role in providing evidence for organic reactions by allowing chemists to analyze the structural changes that occur during a chemical transformation. Spectroscopic techniques, such as infrared (IR) spectroscopy, can identify functional groups present in organic molecules; also, during a chemical reaction, the appearance or disappearance of certain peaks in the IR spectrum can indicate the formation or consumption of specific functional groups, providing evidence for the reaction.[40] Even nuclear magnetic resonance (NMR) spectroscopy can be used to monitor the progress of a reaction in real-time. By taking NMR spectra at different time intervals during a reaction, chemists can observe changes in the chemical shifts and multiplicities of certain nuclei, which can provide insights into the formation of new products or intermediates. NMR spectroscopy provides detailed information about the connectivity and stereochemical nature of organic molecules.[41] Ultimately, by making it possible to identify, characterize, and track chemical changes at the molecular level, spectroscopy is a potent tool for providing evidence for organic reactions.

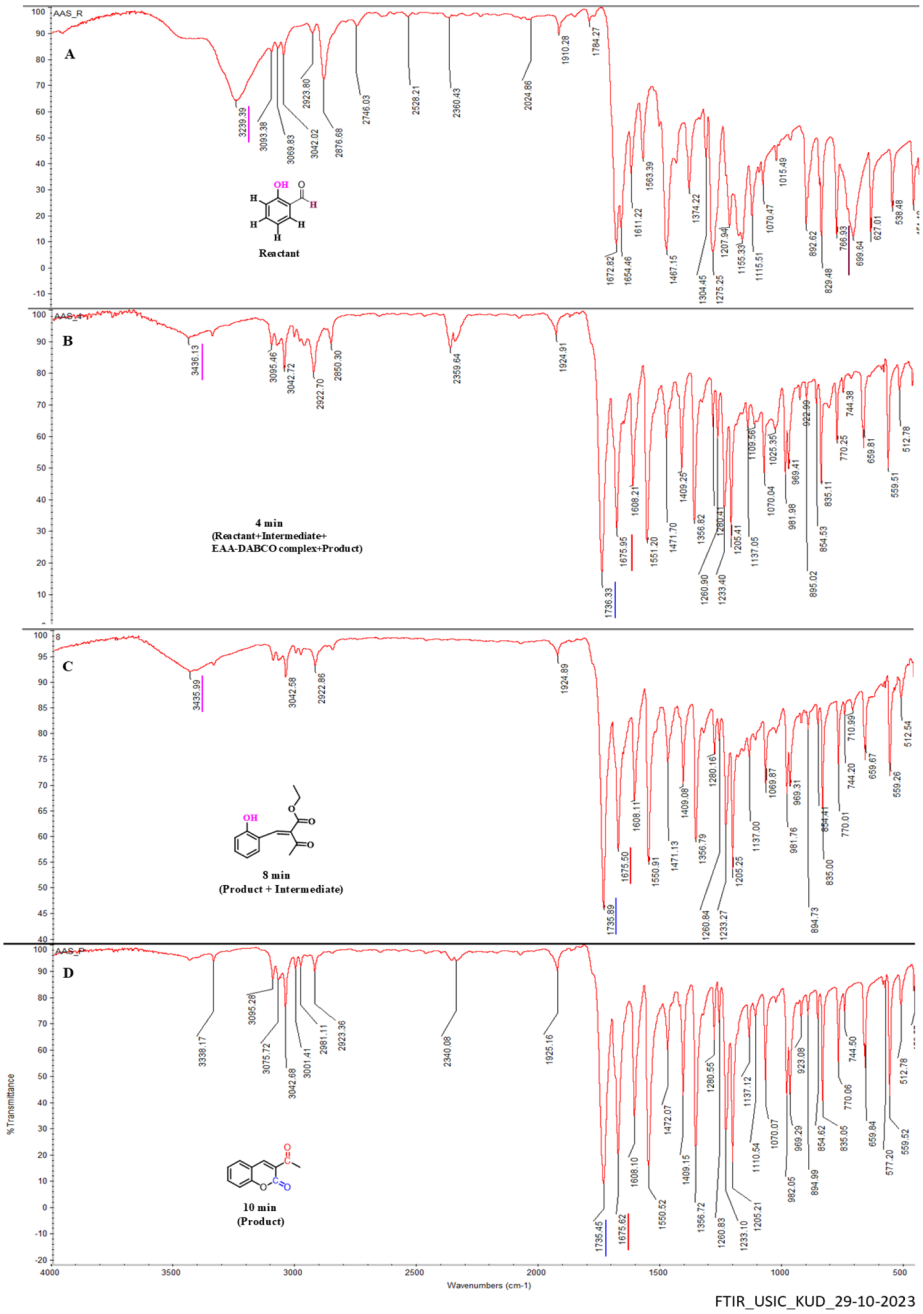

Fig. 8 Plot of % transmittance *vs.* wavenumber for IR spectral analysis as a time-dependent study.

There is a wide variety of intramolecular interaction that affect infrared group frequencies and band intensities. The important intra molecular factors are mass effects, electric effects (inductive and resonance effects), hydrogen bonding, symmetry, conjugation, bond angle strain, field effects, and vibrational coupling effects.[42] The effects of intramolecular interactions in the infrared spectra of molecules make it possible to investigate different types of structural problems. Here, we utilized observations of the reaction changes happening by considering the peak intensities and values. We have focussed mainly on phenolic –OH, C=O, and aldehydic CH stretching frequencies; wherein, salicylaldehydes' aldehydic C=O was observed at 1672 cm^{-1} (Fig. 8A), while at 4th to 8th min two C=O band frequencies were found at 1736 and 1675 cm^{-1}, which indicate the beginning of the formation of the intermediate structure **Y** and 3-acetyl coumarin. Hence, we rushed towards looking for aldehydic characteristic CH stretching vibration bands, which are generally observed around 2800–2650 cm^{-1}, here as two weak bands in this region. The observed two bands at 2746 cm^{-1} and another at 2876 cm^{-1} for salicylaldehyde (Fig. 8A) disappeared during product formation. We also noticed that the hydrogen deformation vibration band of –CHO group appeared at 766 cm^{-1} (ref. 43) (Fig. 8A). In the IR spectra, the peak intensity diminished slowly

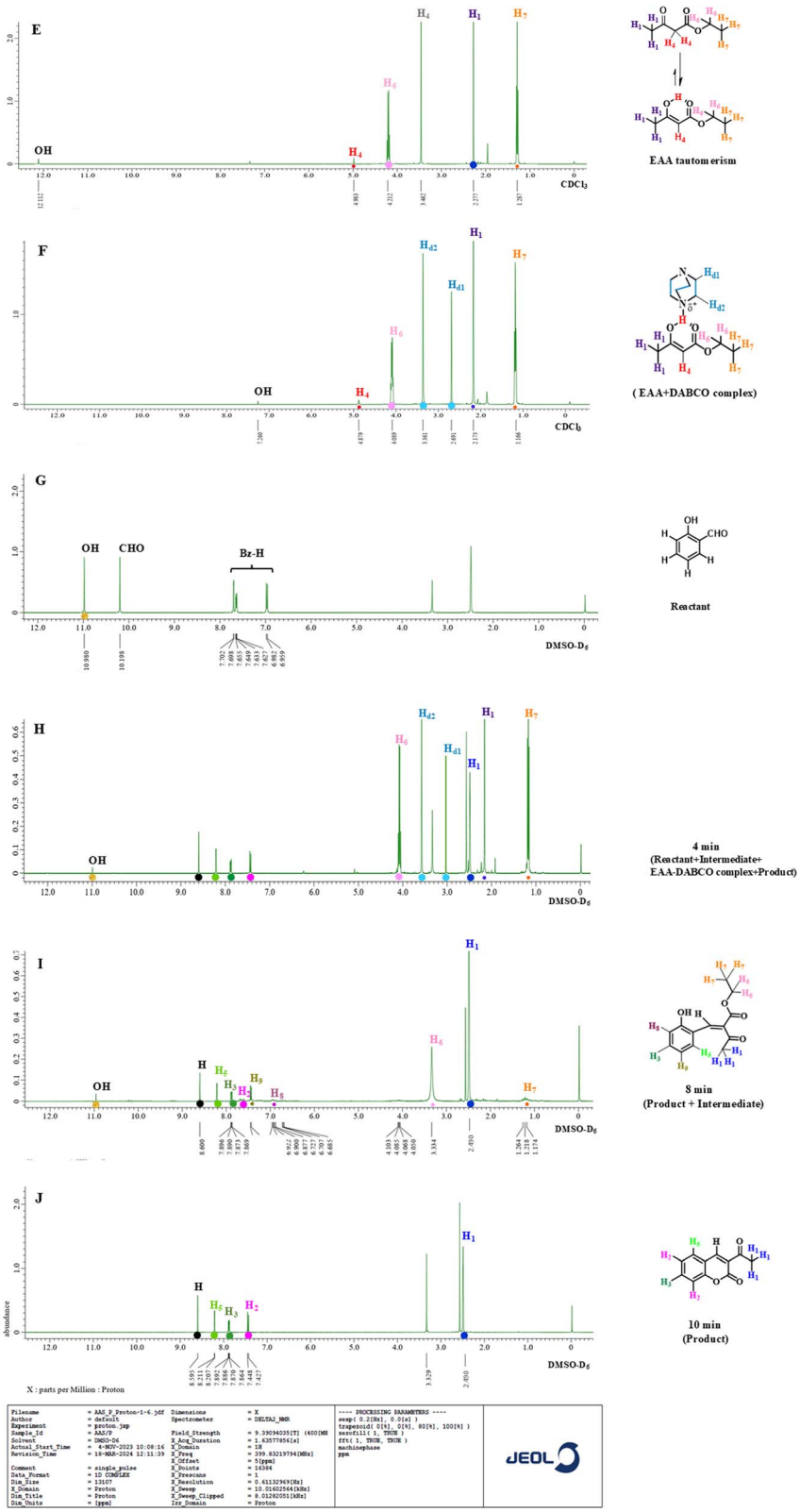

Fig. 9 Plot of abundance *vs.* chemical shift for ^{1}H NMR spectral analysis as a time-dependent study.

as well as a shift of the peak towards higher wavelength was observed, from which we may explain the progress of the reaction up to the 10th min as shown in Fig. 8B–D. Moreover, the IR spectra could only explain the reaction up to a certain extent, but not precisely. Thus, we switched towards studies using time-dependent nuclear magnetic resonance (NMR) from 0 to

10 min. A technique in monitoring structural changes using time-dependent ^{1}H NMR was proposed and then proved. All the components in the reaction, other than DABCO and H_2O, were found to influence the overall kinetics, as proven in the ^{1}H and UV studies. Three sets of standardized reaction conditions were chosen for studying the structural changes occurring in the reaction of salicylaldehyde (1 eq.) upon reaction with EAA (1 eq.) in the presence of the DABCO catalyst (1 eq.) and 1 ml of water at room temperature. Subsequently, these three sets of reactions were performed, quenched at 4, 8, and 10 min, extracted with ethyl acetate, and then the ethyl acetate was removed using a rota vapour technique, leaving behind the isolated compound, which was then analyzed by ^{1}H NMR and compared to the reactants, *i.e.* salicylaldehyde and EAA.

Peaks resonating in the ^{1}H NMR spectrum of pure EAA (Fig. 9E) indicated the presence of both EAA and the enol form of EAA species. While the choice of the perfect analytical tool is a tedious process, choosing right enables getting precise answers. As a result, we were able to tackle the issue caused in ^{1}H NMR with the proton integration values with the use of CV. As shown in Fig. 11C3, two reductive peaks appeared in the CV for EAA caused by the formation of the two enol forms **E1** and **E2**, respectively (see Fig. 7, Phase Ia), and these forms are impossible to distinguish using only the NMR technique. The feasibility of two H_4 peaks at 4.983 (with tautomerism) and 3.462 ppm (without tautomerism) (see Fig. 7, Phase Ia) shows the reversible nature of EAA.[44] For arresting this reversibility of tautomerism in EAA, a bicyclic tertiary amine base DABCO was used which holds the acidic proton of the keto-enol form, thereby making a stable six-membered ring '**X**' (Fig. 7, Phase Ib), as proved by the disappearance of the H_4 peak at 3.462 ppm and appearance of two magnetically equivalent peaks of DABCO at 3.361 and 2.691 ppm in the ^{1}H NMR spectrum, as shown in Fig. 9F. Also, the formation of **X** was the fastest step, as determined through ^{1}H NMR and CV.

The Knoevenagel condensation reaction happens between the aldehydic functional group of salicylaldehyde with the EAA-DABCO complex, resulting in the formation of intermediate '**Y**', namely ethyl 2-(2-hydroxybenzylidene)-3-oxobutanoate (Fig. 7, Phase II). A close examination of the ^{1}H NMR spectra allowed us to conclude that the product formation began as early as 4 min, as can be seen from Fig. 9H with the peaks for H_4 and H_1 resonating at 4.879 and 2.490 ppm, as well as the presence of an intermediate **Y** represented by H_1 at 2.173, while the EAA-DABCO complex represented by H_{d2}, H_{d1} at 3.361 and 2.691 ppm appeared at up to the 4th min. Interestingly, at the 8th min, a disappearance of H_1 (2.173 ppm) was noted, wherein H_{d1} and H_{d2} peaks were observed, and the presence of the phenolic –OH group in intermediate **Y** was observed through the ^{1}H NMR data around 11 ppm, as shown in Fig. 9I. Thus, the intermediate formation was the slowest rate-determining step in the reaction k_2.[45]

Intramolecular ring closure of the phenolic –OH with the ethyl ester part of intermediate **Y** was found to be fastest step $\mathbf{k_3}$ in the reaction. By keenly observing the ^{1}H NMR spectra at the 10th min (Fig. 9J), the reaction was found to be complete, showing only the product 3-acetyl coumarin peaks with the disappearance of the phenolic OH, H_6, H_7, H_8, and H_9 peaks of the intermediate at the 10th min.

Cyclic voltammeter study

Nowadays, electroanalytical methods are well recognized and applied in many chemical fields. Their typical applications include the investigation of redox processes, the study of electrochemical reactions between ions and the surface atoms of electrodes, studies to comprehend reaction intermediates and the stability of reaction products, the qualitative description of electrode reaction mechanisms, and qualitative determination of the characteristics of the charge–transfer reactions between electrolyte ions and electrons from the electrode surface.[46] Since, the current in a circuit is proportional to the electrode's surface area, it is possible to measure the rate of reaction simply by measuring the current flowing through the circuit, using the formula $I = dQ/dt$; therefore, the rate of reduction or oxidation

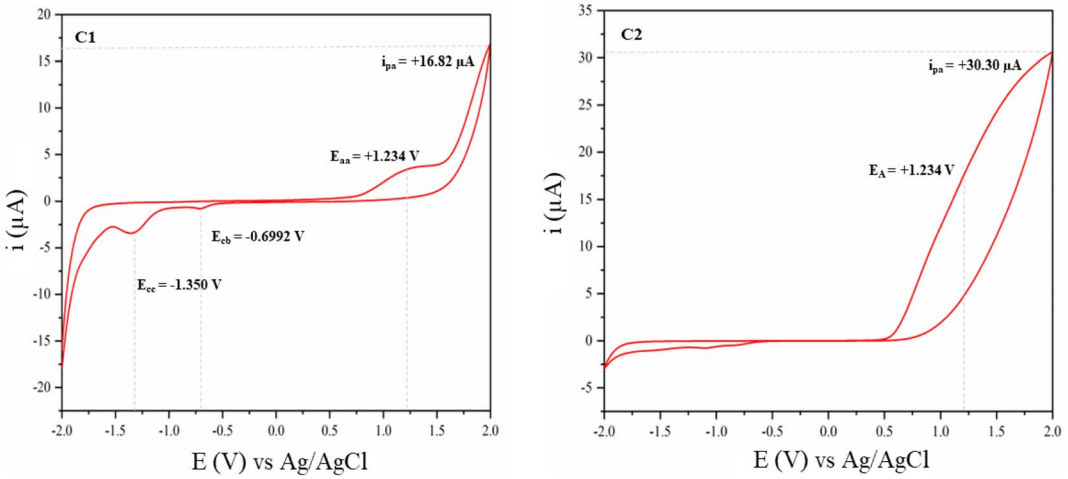

Fig. 10 Plot of the current *vs.* potential: C1 represents the quasi-reversible tautomerism of EAA, C2 represents the arrested form of EAA–DABCO – a favoured irreversible reaction.

at the electrode surface can be determined by the current. Numerous other elements also affect this current, primarily the concentration of the redox species, the electrode's size, shape, and material, the solution resistance, the cell volume, and the quantity of electrons transported.[47]

Spontaneity and stability of tautomerism in EAA and its complex with DABCO catalyst

In order to equate the kinetic and thermodynamic results, cyclic voltammetry was employed, as this allows determining quick electron transfer from a molecule and allows predicting the mechanism of a reaction. In our work, we used Ag/AgCl in 1 M KCl as the reference electrode, platinum electrode as the counter electrode, and a glassy carbon electrode as the working electrode, because it was found that, at this surface (as opposed to metal electrodes such as Ag, Au, Hg, and Pt), voltammetry suffers the least interferences from adsorption processes.[48] Accordingly, the reactions performed so far were chosen, and we prepared two sets of standardized solutions: EAA (1 eq.) dissolved in 10 ml phosphate buffer solution of pH 7 and another same set in the presence of DABCO catalyst (1 eq.).

As is well known, EAA having α-H_4 is more acidic and undergoes tautomerism very quickly and reversibly.[49] We proved this reversible nature of EAA by using cyclic voltammetry. Initially, the potential was scanned linearly over time; wherein, the potential reaches a suitably negative or positive potential, and chemical species undergo oxidation or reduction at the electrode surface, producing an electrical current. This current is monitored during the process of the potential scan in order to figure out how much of a chemical species is undergoing a redox reaction per unit time. The current increases as the potential rises through the redox-active species' half-wave potential ($E_{1/2}$), making oxidation more thermodynamically favourable. Eventually, however, the oxidation process is limited by species diffusion to the electrode surface, resulting in a diffusional tail marked by a drop in current. After that, the electrode's potential sweep is reversed and scanned in the other direction until the starting potential is attained.[50] For a chemically reversible electron-transfer process as denoted in Fig. 7, *i.e.* Phase I without the DABCO catalyst, the reduction of the electrochemically generated species resulted in a cathodic (reductive) current, leading to the voltammogram at a scan rate of 50 mV s^{-1} displayed in Fig. 10C1. The features of cyclic voltammograms that are generally reported in the literature are the anodic and cathodic peak heights, i_{pa} and i_{pc}, and the peak separation ΔE_p. For an electrochemically reversible process, $E_{1/2}$ is measured as halfway between the anodic and cathodic peak potentials. Here, one anodic peak around $E_A = +1.234$ V and two mesmerising cathodic peaks around $E_{CB} = -0.6992$ V and $E_{CC} = -1.350$ V were observed and distinguished by CV only rather than by the NMR technique; this reveals the tautomerism of acidic α-H_4 occurring on either side, in which tautomerism occurring at the keto carbonyl is more favoured (E_{CC}) than at the ester carbonyl (E_{CB}), as judged based on the peak area. The peak to peak separation $\triangle E_{p1} = E_{aa} - E_{cb} = +1.933$ V and $\triangle E_{p2} = E_{aa} - E_{cc} = +2.584$ V reveal the quasi-reversible nature of the reaction.[51] For arresting this reversibility of tautomerism in EAA, a bicyclic tertiary amine base DABCO was used, which holds the acidic proton of the keto-enol form, thereby making a stable six-membered ring '**X**', as proved and shown in Fig. 7, Phase Ib, leading to the voltammogram at a scan rate of 50 mV s^{-1} displayed in Fig. 10C2. The peak around +1.234 V remained while the two reductive peaks vanished; also the height of these peaks $\approx i_{pa}/i_{pc} \neq 1$; which explains the most favoured irreversible reaction.[52] Meanwhile, it was also observed that this step was the fastest step $k1$ (Fig. 7), as confirmed by CV (Fig. 10) and ^{1}H NMR (Fig. 9). Curiosity prompted us to also observe the current intensity peak, whereby the intensity was increased for EAA–DABCO complex (+30.30 μA) over EAA (+16.82 μA) (see Fig. 10C1

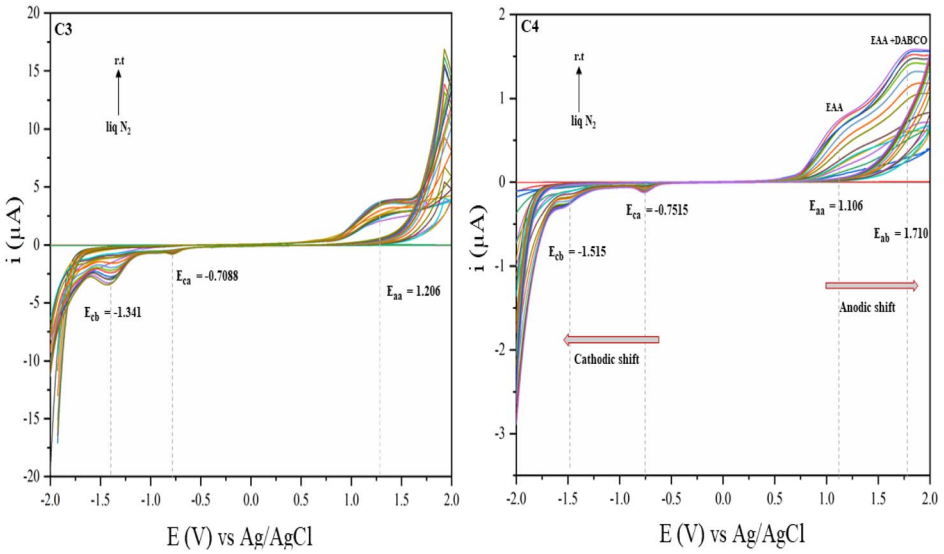

Fig. 11 Plot of the current *vs.* potential, where C3 represents the quasi-reversible tautomerism of EAA, and C4 represents the quasi-reversible tautomerism of EAA in the presence of a non-stoichiometric amount of DABCO.

and C2); which proves that oxidation was more thermodynamically favourable with the formation of a stable complex.

Effect of temperature over tautomerism in EAA and its complex with DABCO catalyst

Despite its significance, insufficient research has been conducted on the impact of temperature on the kinetic behaviour, leading to a lack of conclusive findings.[53] Fig. 11 illustrates the typical CV voltammograms at a scan rate of 50 mV s^{-1} for two different sets of solutions of EAA (1 eq.) and another same set in the presence of DABCO catalyst (0.0125 eq.).

The electron mobility/shift in the α-H_4 acidic proton of EAA was examined (Fig. 11C3) under liquid N_2 to room temperature. It was found that the tautomerism stopped in liquid N_2 atmosphere and that the mesomeric effect slowing began from −10 °C with raising the temperature, which could be detected by an increase in the current. All the separations between the oxidation and reduction peak potentials ($\triangle E_p$) could be observed in Fig. 11C3 and were much greater than 60 mV, indicating a quasi-reversible reaction.

In order to examine the displacement of the potential (V) of the anodic and cathodic shifts and also the intensity of the oxidative current peak during the EAA–DABCO complexation reaction, a non-stoichiometric experimental proportion of DABCO was taken. The anodic peak of pure EAA around E_{aa} = 1.206 V (Fig. 11C3) was shifted to E_{aa} = 1.106 V (Fig. 11C4), implying the formation of a complex was beginning and a new peak could thus be observed for the EAA–DABCO complex around E_{ab} = 1.710 V. Similarly, the complexation of EAA–DABCO caused a shift in the cathodic peak of EAA around E_{ca} = −0.7088 V (Fig. 11C3) to E_{aa} = −0.7515 V (Fig. 11C4) upon complexation. Second, the reductive peak abruptly changed and shifted to E_{cb} = −1.515 V (Fig. 11C4), revealing that the tautomerism of acidic α-H_4 occurred on either side, in which the tautomerism occurring at the keto carbonyl was favoured (E_{cb}) over that on the ester carbonyl (E_{ca}), as judged based on the peak area. Furthermore, the vanishing of both the anodic and cathodic peaks of EAA upon the perfect stoichiometric complexation with DABCO was studied.

Effect of DABCO concentration over tautomerism of EAA – until the favoured irreversible process

Fig. 12 illustrates the typical CV voltammograms at a scan rate of 50 mV s^{-1} for varying concentrations of DABCO on EAA tautomerism solution in 10 ml phosphate buffer at pH 7. Here, it can be seen that the anodic peak current (i_{pa}) increased as the concentration of the DABCO catalyst increased. We were curious enough to check the cyclic voltammogram for each concentration, which discloses two distinct observations: first, the oxidation peak pattern changed with increasing the peak current as the concentration of DABCO increased, indicating the more thermodynamically favourable formation of a stable complex. Second, the reduction peak decreased with increasing the concentration of DABCO and straightened precisely at 1 eq. concentration, indicating the conversion of a quasi-reversible to an irreversible process. Consequently, 1 eq. DABCO concentration was the optimal quantity to hold the complete enol form of EAA–DABCO, making it irreversible by complexing.

Experimental

General information

All the reactions were monitored by TLC (Merck silica gel F-254 plates) and the isolated products were characterized by FTIR (KBr pellets; dated 29-10-2023), and ^{1}H NMR (400 MHz; dated 04-11-2023) respectively. Chemical shifts were reported in parts per million (ppm) downfield from the TMS internal standard. Electrochemical investigations were carried out on a CHI6134E

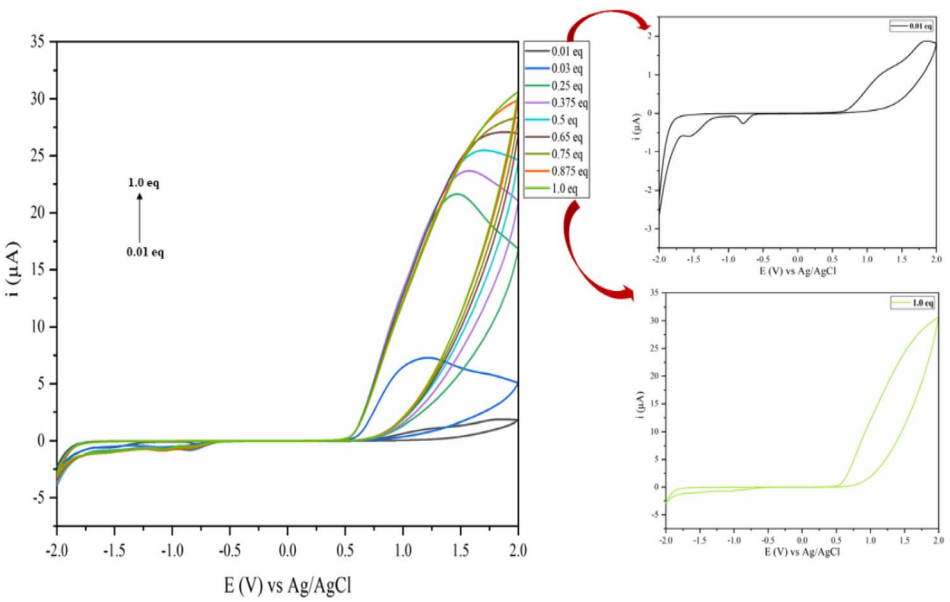

Fig. 12 Plot of the current *vs.* potential showing the conversation of the quasi-reversible to an irreversible process with increasing the concentration of DABCO (from 0.0125 to 1 eq.).

electrochemical analyzer with a standard three-electrode cell set-up (CH Instruments Ltd Co., USA).

General procedure for the synthesis of 3-acetylcoumarins (3a–h)

A mixture of EAA (1 eq.), substituted *o*-hydroxyaldehydes (1 eq.), and catalyst (DABCO, DABCO- ionic liquids) was stirred at room temperature until TLC monitoring analysis indicated (10–20 min) that the reaction was complete. The solid that separated was filtered and washed thoroughly with water.

Procedure for recovering of the DABCO catalyst and ethanol

Following the general procedure described above, initially, the filtrate obtained was taken and distilled under reduced pressure to recover ethanol. Moreover, the aqueous solution containing only the catalyst and free from ethanol was reused once again for the reaction. The catalyst could be reused at least 5 times.

Conclusions

From this investigation, we have shown a most useful facile green synthesis of 3-acetylcoumarins for the first time in water, offering high purity and yield under mild conditions. The condensation reaction worked well with a stoichiometric amount of catalyst in aqueous medium at room temperature. This methodology offers a good scope for the synthesis of a wide variety of 3-acetylcoumarins compared to earlier reported approaches. Also, the catalysts DABCO and DABCO-ionic liquids could be easily recovered and reused more efficiently. Meanwhile, the by-product ethanol could also be recovered and used wherever essential. We demonstrated the effect of the DABCO catalyst/reactants on the rate kinetics of the reaction and thermodynamic activation parameters. From these studies, it was revealed that the DABCO catalyst initiates the reaction very quickly and completes the reaction *via* holding the tautomerism, by EAA-DABCO complexation. While the interesting step of EAA-DABCO complexation and its involvement in the progress of the reaction were determined through FT-IR and time-dependent ^{1}H NMR studies. More interestingly for the first time, the tautomeric form of EAA and its complexation with DABCO were studied in detail through CV, suggesting that the tautomerism of EAA happens fast, whereas in the EAA–DABCO complex tautomerism was arrested, leading to completion of the reaction in a shorter time. The salient features of this method are its totally eco-friendly condition, the reusability of the catalyst and by-product, and it is more economical. Moreover, this protocol can be used for the large-scale synthesis of substituted-3-acetylcoumarins; thus, the present procedure is a significant improvement over existing methods. More broadly, the exploration of this remarkable method may lead to new condensation reactions.

Data availability

The authors confirm that the data supporting the findings of this study are available within the article.

Author contributions

AAS conceived the ideas and carried out the experiments. SLS and LAS were involved in research investigation. All three authors contributed to the manuscript.

Conflicts of interest

There are no conflicts to declare.

Acknowledgements

The authors acknowledge the University Scientific Instrumentation centre (USIC) and DST-SAIF, Karnatak University, Dharwad for spectral analysis. One of the author Arpita A. Shanbhag is thankful to URS (Sr. No./KU/Fellowship/URS/2022/376 dated: 18/09/2022) and CSIR-NET- JRF New Delhi (File. No. 09/0101(15285)/2022-EMR-I dated: 27/07/2022) for the financial support. The authors express their gratitude towards Dr Atmanand Bagoji and Dr Amar Durgannavur for their valuable advice and insights.

References

1 S. M. Sethna and N. M. Shah, *Chem. Rev.*, 1945, **36**, 1–62.
2 A. Vogel, *Ann Phys.*, 1820, **64**, 161–166.
3 For general reviews on Pechmann reaction, see:(*a*) T. Sugino and K. Tanaka, *Chem. Lett.*, 2001, 110; (*b*) A. Hegedüs and Z. Hell, *Catal. Lett.*, 2006, **112**, 105–108; (*c*) S. Sethna and P. Ragini, *Org. React.*, 2004, **7**, 1–58; (*d*) N. G. Khaligh, *Catal. Sci. Technol.*, 2012, **2**, 1633–1636; (*e*) L. T. L. Nguyen, K. K. A. Le, H. X. Truong and N. T. S. Phan, *Catal. Sci. Technol.*, 2012, **2**, 521–528; (*f*) H. V. Pechmann and J. B. Cohe, *Eur. J. Inorg. Chem.*, 2015, **17**, 2187–2191; (*g*) G. K. Hodgson, S. Impellizzeri and J. C. Scaiano, *Chem. Sci.*, 2016, **7**, 1314–1321; (*h*) A. K. Gupta, D. De, R. Katoch, A. Garg and P. K. Bharadwaj, *Inorg. Chem.*, 2017, **56**, 4697–4705.
4 For general reviews on Knoevenagel reaction, see:(*a*) G. Brufola, F. Fringuelli, O. Piermatti and F. Pizzo, *ChemInform*, 1996, **27**, DOI: **10.1002/CHIN.199643107**; (*b*) L. T. L. Nguyen, K. K. A. Le, H. X. Truong and N. T. S. Phan, *Catal. Sci. Technol.*, 2012, **2**, 521–528; (*c*) J. J. Clemens, J. L. Asgian, B. B. Busch, T. Coon, J. Ernst, L. Kaljevic, P. J. Krenitsky, T. D. Neubert, E. J. Schweiger, A. Termin and D. Stamos, *J. Org. Chem.*, 2013, **78**, 780–785; (*d*) P. Rammohan and S. Taradas, *Int. J. Org. Chem.*, 2014, **04**, 106–115; (*e*) R. H. Vekariya and H. D. Patel, *Synth. Commun.*, 2014, **44**, 2756–2788; (*f*) J. V. Schijndel, L. A. Canalle, J. Smid and J. Meuldijk, *Open J. Phys. Chem.*, 2016, **06**, 101–108; (*g*) R. C. M. A. Sobrinho, P. M. de Oliveira, C. R. M. D'Oca, D. Russowsky and M. G. M. D'Oca, *RSC Adv.*, 2017, **7**, 3214–3221; (*h*) S. Crotti, N. Di Iorio, C. Artusi, A. Mazzanti, P. Righi and G. Bencivenni, *Org. Lett.*, 2019, **21**, 3013–3017; (*i*) A. Hasija, V. Prakash, M. S. Prakash, G. Krishnasamy and D. Chopra, *Cryst. Struct. Theory Appl.*, 2020, **09**, 49–62.

5 For general reviews on Perkin reaction, see:(*a*) J. R. Johnson, *Org. React.*, 1942, **1**, 210–265; (*b*) O. Yoshiro and M. Tsuchida, *J. Org. Chem.*, 1959, **24**, 78–83; (*c*) P. M. Pawar, K. J. Jarag and G. S. Shankarling, *Green Chem.*, 2011, **13**, 2130–2134.

6 For general reviews on Reformatsky reaction, see:(*a*) M. Á. Fernández-Ibáñez, B. Maciá, A. J. Minnaard and B. L. Feringa, *Chem. Commun.*, 2008, 2571–2573; (*b*) R. L. Shriner, *Org. React.*, 2011, DOI: 10.1002/0471264180.or001.01; (*c*) C. Wolf and M. Moskowitz, *J. Org. Chem.*, 2011, **76**, 6372–6376; (*d*) A. Maestro, E. Martinez De Marigorta, F. Palacios and J. Vicario, *Org. Lett.*, 2019, **21**, 9473–9477; (*e*) Qi-L. Chen, Le Mao, Yi-F. Pan, H. Cai, X.-M. Zhang, Fu-M. Zhang, Ai-J. Ma, J.-B. Peng and Y.-Q. Tu, *Chem. Commun.*, 2023, **59**, 14427–14430.

7 For general reviews on Wittig reaction, see:(*a*) N. S. Narasimhan and R. S. Mali, *Tetrahedron*, 1975, **31**, 1005–1009; (*b*) T. Harayama, K. Nakatsuka, H. Nishioka, K. Murakami, Y. Ohmori, Y. Takeuchi, H. Ishii and K. Kenmotsu, *Heterocycles*, 1994, **38**, 2729–2738; (*c*) I. Yavari, R. H. Shoar and A. Zonouzi, *Tetrahedron Lett.*, 1998, **39**, 2391–2392; (*d*) P. J. Murphy and S. E. Lee, *J. Chem. Soc., Perkin Trans. 1*, 1999, **1**, 3049–3066; (*e*) R. Robiette, J. Richardson, V. K. Aggarwal and J. N. Harvey, *J. Am. Chem. Soc.*, 2006, **128**, 2394–2409; (*f*) J. Zheng, J. Cai, J. H. Lin, Y. Guo and J. C. Xiao, *Chem. Commun.*, 2013, **49**, 7513–7515; (*g*) P. A. Byrne and D. G. Gilheany, *Chem. Soc. Rev.*, 2013, **42**, 6670–6696; (*h*) D. Reiter, P. Frisch, T. Szilvási and S. Inoue, *J. Am. Chem. Soc.*, 2019, **141**, 16991–16996; (*i*) A. B. Cuenca and E. Fernández, *Chem. Soc. Rev.*, 2021, **50**, 72–86; (*j*) A. M. Borys, E. F. Rice, G. S. Nichol and M. J. Cowley, *J. Am. Chem. Soc.*, 2021, **143**, 14065–14070.

8 V. M. Alexander, R. P. Bhat and S. D. Samant, *Tetrahedron Lett.*, 2005, **46**, 6957–6959.

9 For a reviews on coumarin synthesis by organopalladium intermediates, see:(*a*) C. Jia, D. Piao, T. Kitamura and Y. Fujiwara, *J. Org. Chem.*, 2000, **65**, 7516–7522; (*b*) C. Jia, D. Piao, J. Oyamada, W. Lu, T. Kitamura and Y. Fujiwara, *Science*, 2000, **287**, 1992–1995; (*c*) S. Aoki, C. Amamoto, J. Oyamada and T. Kitamura, *Tetrahedron*, 2005, **61**, 9291–9297; (*d*) B. Gabriele, R. Mancuso, G. Salerno and P. Plastina, *J. Org. Chem.*, 2008, **73**, 756–759; (*e*) T. D. A. Fernandes, B. Gontijo Vaz, M. N. Eberlin, A. J. M. Da Silva and P. R. R. Costa, *J. Org. Chem.*, 2010, **75**, 7085–7091; (*f*) K. Sasano, J. Takaya and N. Iwasawa, *J. Am. Chem. Soc.*, 2013, **135**, 10954–10957; (*g*) S. Dharani, G. Kalaiarasi, D. Sindhuja, V. M. Lynch, R. Shankar, R. Karvembu and R. Prabhakaran, *Inorg. Chem.*, 2019, **58**, 8045–8055.

10 For a reviews on derivatives of coumarin application in laser dyes, see:(*a*) M. S. A. Abdel-Mottaleb, M. S. Antonious, M. M. Abo-Ali, L. F. M. Ismail, B. A. El-Sayed and A. M. K. Sherief, 1992, DOI:DOI: 10.1007/BF02863363; (*b*) M. S. A. Abdel-Mottaleb, M. S. Antonious, M. M. Abo-Aly, L. F. M. Ismaiel, B. A. El-Sayed and A. M. K. Sherief, *J. Photochem. Photobiol., A*, 1989, **50**, 259–273; (*c*) C. Eggeling, L. Brand and C. A. M. Seidel, *Bioimaging*, 1997, **5**, 105–115; (*d*) J. H. Richardson, L. L. Steinmetz, S. B. Deutscher, W. A. Bookless and W. L. Schmelzinger, *Z. Naturforsch. A*, 1978, **33**, 1592–1593; (*e*) J. R. Mannekutla, B. G. Mulimani and S. R. Inamdar, *Spectrochim. Acta, Part A*, 2008, **69**, 419–426; (*f*) S. A. Azim, S. M. Al-Hazmy, E. M. Ebeid and S. A. El-Daly, *Opt. Laser Technol.*, 2005, **37**, 245–249; (*g*) A. Fischer, C. Cremer and E. H. K. Stelzer, *Appl. Opt.*, 1995, **34**(12), 1989–2003.

11 Z. Xu, X. Liu, J. Pan and D. R. Spring, *Chem. Commun.*, 2012, **48**, 4764–4766.

12 For a reviews on derivatives of coumarin application in solution dynamic probes, see:(*a*) N. M. Correa and N. E. Levinger, *J. Phys. Chem. B*, 2006, **110**, 13050–13061; (*b*) J. A. Gutierrez, R. D. Falcone, J. J. Silber and N. M. Correa, *J. Phys. Chem. A*, 2010, **114**, 7326–7330.

13 For a reviews on derivatives of coumarin application in dye-sensitized solar cell, see: (*a*) K. Hara, K. Sayama, Y. Ohga, A. Shinpo, S. Suga and H. Arakawa, *Chem. Commun.*, 2001, 569–570; (*b*) K. Hara, Z. S. Wang, T. Sato, A. Furube, R. Katoh, H. Sugihara, Y. Dan-Oh, C. Kasada, A. Shinpo and S. Suga, *J. Phys. Chem. B*, 2005, **109**, 15476–15482; (*c*) Z. S. Wang, Y. Cui, K. Hara, Y. Dan-Oh, C. Kasada and A. Shinpo, *Adv. Mater.*, 2007, **19**, 1138–1141; (*d*) Z. S. Wang, Y. Cui, Y. Dan-oh, C. Kasada, A. Shinpo and K. Hara, *J. Phys. Chem. C*, 2007, **111**, 7224–7230.

14 For a reviews on derivatives of coumarin application in fluorescence brightner, see:(*a*) N. S. Naik, L. A. Shastri, C. Bathula, B. Chougala, S. Shastri, M. Holiyachi and V. Sunagar, *J. Fluoresc.*, 2017, **27**, 419–425; (*b*) S. Samundeeswari, M. V. Kulkarni, J. Yenagi and J. Tonannavar, *J. Fluoresc.*, 2017, **27**, 1247–1255.

15 A. V Shanbhag, T. V Venkatesha, R. A. Prabhu and B. M. Praveen, *Bull. Mater. Sci.*, 2011, **34**(3), 571–576.

16 For a reviews see:(*a*) M. K. Li, J. Li, Y. Zhou, X. Y. Xue, X. Shi, Z. Y. Tu, Z. Hou and X. X. Luo, *Res. Chem. Intermed.*, 2015, **41**, 3289–3296; (*b*) E. Mansour, E. M. Nassar, A. F. El-Farargy and F. M. Abdelrazek, *Russ. J. Bioorg. Chem.*, 2020, **46**, 582–589.

17 V. N. Toan and N. D. Thanh, *Med. Chem.*, 2021, **30**, 1868–1885.

18 For a reviews see:(*a*) M. L. Low, G. Paulus, P. Dorlet, R. Guillot, R. Rosli, N. Delsuc, K. A. Crouse and C. Policar, *BioMetals*, 2015, **28**, 553–566; (*b*) M. Mahdavi, S. Mohammadi-Izad, M. Saeedi, M. Safavi, S. E. S. Ebrahimi, A. Foroumadi and A. Shafiee, *J. Iran. Chem. Soc.*, 2016, **13**, 1139–1144; (*c*) J. B. Foo, M. L. Low, J. H. Lim, Y. Z. Lor, R. Zainol Abidin, V. Eh Dam, N. Abdul Rahman, C. Y. Beh, L. C. Chan, C. W. How, Y. S. Tor and L. Saiful Yazan, *BioMetals*, 2018, **31**, 505–515.

19 V. Channabasappa, K. Kumara and A. Kumar Kariyappa, *J. Chem. Sci.*, 2021, **133**, 130.

20 P. Aragade, M. Palkar, P. Ronad and D. Satyanarayana, *Med. Chem. Res.*, 2013, **22**, 2279–2283.

21 (*a*) N. Ingale, V. Maddi, M. Palkar, P. Ronad, S. Mamledesai, A. H. M. Vishwanathswamy and D. Satyanarayana, *Med. Chem. Res.*, 2012, **21**, 16–26; (*b*) N. Hosseini Nasab, F. Azimian, H. G. Kruger and S. J. Kim, *Arabian J. Chem.*, 2023, **16**, 104472.

22 J. K. Gupta, P. K. Sharma, R. Dudhe, A. Chaudhary, A. Singh, P. K. Verma, S. C. Mondal, R. K. Yadav and S. Kashyap, *Med. Chem. Res.*, 2012, **21**, 1625–1632.
23 A. M. Msa and M. S. Attia, *Res. J. Chem. Sci.*, 2013, **3**, 4.
24 (*a*) A. S. Lunkad and R. L. Sawant, *Int. J. Pharm. Sci. Res.*, 2018, **9**, 2852–2858; (*b*) D. Bogdal, *J. Chem. Res.*, 1998, 468–469; (*c*) K. V. Sashidhara, A. Kumar, M. Kumar, R. Sonkar, G. Bhatia and A. K. Khanna, *Bioorg. Med. Chem. Lett.*, 2010, **20**, 4248–4425; (*d*) O. O. Ajania and O. C. Nwinyi, *J. Heterocycl. Chem.*, 2010, **47**, 179; (*e*) T. A. Hamlin and N. E. Leadbeater, *J. Visualized Exp.*, 2015, **105**, DOI: 10.3791/52393.
25 (*a*) J. S. Ghomi and Z. Akbarzadeh, *Ultrason. Sonochem.*, 2018, **40**, 78–83; (*b*) B. V. Kumar, H. S. B. Naik, D. Girija and B. Vijayakumar, *J. Chem. Sci.*, 2011, **123**, 615–621.
26 (*a*) D. Khan, S. Mukhtar, M. A. Alsharif, M. I. Alahmdi and N. Ahmed, *Tetrahedron Lett.*, 2017, **58**, 3183–3187; (*b*) T. N. Lieu, K. D. Nguyen, D. T. Le, T. Truong and N. T. S. Phan, *Catal. Sci. Technol.*, 2016, **6**, 5916–5926.
27 (*a*) S. B. Phadtare and G. S. Shankarling, *Environ. Chem. Lett.*, 2012, **10**, 363–368; (*b*) P. Verdía, F. Santamarta and E. Tojo, *Molecules*, 2011, **16**, 4379–4388.
28 (*a*) K. N. Nandkishor, G. Sumit, V. Shinde, V. Sandeep and N. W. Jadhav, *Chin. J. Chem.*, 2007, **25**, 1687; (*b*) X. You, H. Yu, M. Wang, J. Wu and Z. Shang, *Lett. Org. Chem.*, 2012, **9**, 19–23.
29 S. S. Gholap, U. P. Deshmukh and M. S. Tambe, *Iran. J. Catal.*, 2013, **3**, 171–176.
30 M. M. Heravi, S. Sadjadi, H. A. Oskooie, R. H. Shoar and F. F. Bamoharram, *Catal. Commun.*, 2008, **9**, 470–474.
31 (*a*) M. Li, R. Zhang, C. Jia, Z. Liu, Y. Liu and A. Ying, *Fuel*, 2024, **375**, 132671; (*b*) X. Lu, S. Li, L. Wang, S. Huang, Z. Liu, Y. Liu and A. Ying, *Fuel*, 2022, 122318; (*c*) S. Li, X. Lu, Q. Liu, L. Wang, Y. Liu, Z. Liu and A. Ying, *J. Mater. Chem. A*, 2022, **10**, 3531–3542; (*d*) A. Ying, S. Li, X. Liu, J. Wang, Y. Liu and Z. Liu, *J. Catal.*, 2020, **391**, 312–326; (*e*) N. Seyedi, F. Shirini and H. Tajik, *J. Mol. Struct.*, 2023, **1285**, 135547; (*f*) P. P. Foumani, M. Mousapour, F. Shirini, H. Tajik and S. Hassanpoor, *J. Iran. Chem. Soc.*, 2023, **2**, 359–371; (*g*) N. Seyedi, L. N. Nasyrmahale, F. Shirini and H. Tajik, *ChemistrySelect*, 2023, **8**, e202204306; (*h*) N. M. Shaikh, V. Adimule, G. B. Bagihalli and R. S. Keri, *Top. Catal.*, 2022, 1–10; (*i*) S. Sahrapeyma, F. Shirini and M. Mamaghani, *Iran. J. Sci.*, 2023, **47**, 1553–1564; (*j*) M. Dhama, P. Gupta and D. Sah, *Res. Chem. Intermed.*, 2024, **50**, 575–595; (*k*) J. Long, W. Dai, M. Zou, B. Li, S. Zhang, L. Yang, J. Mao, P. Mao, S. Luo and X. Luo, *Microporous Mater.*, 2021, **318**, 111027.
32 F. Scholz, *ChemTexts*, 2015, **1**, 17.
33 For a reviews see: (*a*) Y. Q. Yu and D. Z. Xu, *RSC Adv.*, 2015, **5**, 28857–28863; (*b*) N. Sahiba, A. Sethiya, P. Teli and S. Agarwal, *ACS Omega*, 2023, **8**, 5877–5884.
34 B. Baghernejad and M. Fiuzat, *Eurasian Chem. Commun.*, 2020, **2**, 1088–1092.
35 (*a*) K. R. Seddon, A. Stark and M. J. Torres, *Pure Appl. Chem.*, 2000, **72**, 2275–2287; (*b*) M. J. Earle and K. R. seddon, *Pure Appl. Chem.*, 2000, **72**, 1391–1398; (*c*) P. Wasserscheid and T. Welton, *Org. Process Res. Dev.*, 2003, **7**, 223–224; (*d*) S. Zhang, N. Sun, X. He, X. Lu and X. Zhang, *J. Phys. Chem. Ref. Data*, 2006, **35**, 1475–1517; (*e*) P. Nockemann, B. Thijs, S. Pittois, J. Thoen, C. Glorieux, K. V. Hecke, L. V. Meervelt, B. Kirchner and K. Binnemans, *J. Phys. Chem. B*, 2006, **110**, 20978–20992; (*f*) T. Welton, *Chem. Rev.*, 1999, **8**, 2071–2084.
36 (*a*) H. M. Han, C. R. Lu, Y. Zhang and D. C. Zhang, *Acta Crystallogr., Sect. E: Struct. Rep. Online*, 2005, **E61**, o1864–o1866; (*b*) D. Secci, S. Carradori, A. Bolasco, P. Chimenti, M. Yáñez, F. Ortuso and S. Alcaro, *Eur. J. Med. Chem.*, 2011, **46**, 4846–4852; (*c*) Z. Q. Xiong, L. Yang, S. Z. Xiao, C. Y. Yang and X. L. Nie, *Z. Kristallogr.*, 2022, **237**, 635–637; (*d*) H. Valizadeh, A. Shockravi and H. Gholipur, *J. Heterocycl. Chem.*, 2007, **44**, 867; (*e*) https://www.chembk.com/en/chem/848322-75-8; (*f*) N. N. Korgavkar and S. D. Samant, *New J. Chem.*, 2017, **41**, 12422.
37 C. Reichardt and T. Welton, *Solvents and Solvent Effects in Organic Chemistry*, 4th edn, 2011.
38 F. Carey and R. J. Sundberg, *Advanced Organic Chemistry, Part B: Reactions and Synthesis*, 5th edn, 2007.
39 (*a*) L. Jattinagoudar, S. Nandibewoor, S. Chimatadar and J. Solution, *Chem*, 2016, **45**, 497–517; (*b*) A. M. Bagoji, P. A. Magdum, S. T. Nandibewoor and J. Solution, *Chem*, 2016, **45**, 1715–1728.
40 (*a*) F. Borek, *J. Org. Chem.*, 1961, **26**(4), 1292–1294; (*b*) S. Ghorai, A. Laskin and A. V. Tivanski, *J. Phys. Chem. A*, 2011, **115**, 4373–4380; (*c*) D. T. Bregante, P. Priyadarshini, and D. W. Flaherty, 2017, URL: https://www.sciencedirect.com/science/article/pii/S0021951717300428.
41 (*a*) E. J. Cone, R. H. Garner and A. A. Wallace Hayes, *J. Org. Chem.*, 1972, **37**(26), 4436–4439; (*b*) F. B. Mallory and M. B. Baker, *J. Org. Chem.*, 1984, **49**(8), 1324–1326; (*c*) G. Bellucci, R. Bianchini, C. Chiappe, R. Ambrosetti, D. Catalano, A. J. Bennet, H. Slebocka-Tilk, G. H. M. Aarts and R. S. Brown, *J. Org. Chem.*, 1993, **58**, 3401–3406; (*d*) K. Nilsson, C. Ullenius and N. Krause, *J. Am. Chem. Soc.*, 1996, **118**, 4194–4195; (*e*) C. Puke, G. Erker, B. Wibbeling and R. Fröhlich, *Eur. J. Org Chem.*, 1999, **8**, 1831–1841; (*f*) F. Susanne, D. S. Smith and A. Codina, *Org. Process Res. Dev.*, 2012, **16**, 61–64; (*g*) A. K. Eckhardt, *Chem. Commun.*, 2022, **58**, 8484–8487; (*h*) R. Nagarjuna, A. Thakur, A. Balapure, M. S. M. Saifullah, J. Ray Dutta and R. Ganesan, *Mater. Adv.*, 2023, **5**, 593–607.
42 (*a*) R. C. Lord and F. A. Miller, *Appl. Spectrosc.*, 1956, **115**, 10; (*b*) L. J. Bellamy, "*The Infrared Spectra of Complex Molecules*." Wiley, New York, 1958.
43 (*a*) N. B. Colthup, *J. Opt. Soc. Am.*, 1950, **4**(6), 397; (*b*) A. Ashdown and T. A. Kletz, *J. Chem. Soc.*, 1948, 1454–1456.
44 For a reviews on keto-enol tautomerism see: (*a*) G. Allen and R. A. Dwek, *J. Chem. Soc. B*, 1966, 161–163; (*b*) E. J. Drexler and K. W. Field, *J. Chem. Educ.*, 1976, **53**(6), 392–393; (*c*) Measuring the equilibrium constant of a keto-enol tautomerism using benchtop NMR, Application note AN52327, URL:AN52327-measuring-equilibrium-constant-keto-enol-tautomerism.pdf (thermofisher.com);; (*d*)

M. M. Fokendt, B. E. Weiss-Lopez, J. P. Cbauvel and N. S. True, *J. Phys. Chem.*, 1985, **89**, 3347–3352.

45 E. V. Dalessandro, H. P. Collin, M. S. Valle and J. R. Pliego, *RSC Adv.*, 2016, **6**, 57803–57810.

46 (*a*) R. S. Nicholson and I. Shain, *Anal. Chem.*, 1964, **36**(4), 706–723; (*b*) J. Wang and N. York, *Analytical Electrochemistry*, 2nd edn, 2000.

47 P. S. Joshi and D. S. Sutrave, *Int. J. ChemTech Res.*, 2018, **11**, 77–88.

48 (*a*) R. D. Webster, A. M. Bond and T. Schmidt, *J. Chem. Soc., Perkin Trans. 1*, 1995, **2**, 1365–1374; (*b*) R. D. Webster, *J. Chem. Soc., Perkin Trans. 1*, 1999, **2**, 263–269.

49 (*a*) M. A. Nichols and M. J. Waner, *J. Chem. Educ.*, 2010, **87**, 952–955; (*b*) S. Farmer, D. Kennepohl, L. Morsch and L. Morsch, *Keto-Enol Tautomerism*, 2010, URL: 22.1: Keto-Enol Tautomerism - Chemistry LibreTexts.

50 (*a*) N. Elgrishi, K. J. Rountree, B. D. McCarthy, E. S. Rountree, T. T. Eisenhart and J. L. Dempsey, *J. Chem. Educ.*, 2018, **95**, 197–206; (*b*) C. Sandford, M. A. Edwards, K. J. Klunder, D. P. Hickey, M. Li, K. Barman, M. S. Sigman, H. S. White and S. D. Minteer, *Chem. Sci.*, 2019, **10**, 6404–6422.

51 (*a*) G. Diao and Z. Zhang, *J. Electroanal. Chem.*, 1996, **410**, 155–162; (*b*) A. A. Al Owais, I. S. El-Hallag and E. H. El-Mossalamy, *Int. J. Electrochem. Sci.*, 2022, **17**, 220631.

52 T. Gieshoff, A. Kehl, D. Schollmeyer, K. D. Moeller and S. R. Waldvogel, *J. Am. Chem. Soc.*, 2017, **139**, 12317–12324.

53 (*a*) H. Liu, T. Cai, Q. Song, L. Yang, Q. Xu and C. Yan, *Int. J. Electrochem. Sci.*, 2013, **8**, 2515–2523; (*b*) W. Wang, X. Fan, J. Liu, C. Yan and C. Zeng, *RSC Adv.*, 2014, **4**, 32405–32411.